International Journal of Engineering Science 131 (2018) 80–99

Contents lists available at ScienceDirect

International Journal of Engineering Science

journal homepage: www.elsevier.com/locate/ijengsci

Gradient elasticity theory for fiber composites with fibers resistant to extension and flexure

Chun IL Kim*, Mahdi Zeidi

Department of Mechanical Engineering, University of Alberta, Edmonton, Alberta T6G 2G8, Canada

ARTICLE INFO

Article history:
Received 18 April 2018
Revised 5 June 2018
Accepted 14 June 2018
Available online 3 July 2018

Keywords:
Finite plane deformations
Fiber-reinforced materials
Bidirectional fiber
Superposed incremental deformations
Flexure
Plane bias extension

ABSTRACT

A model for the mechanics of an elastic solid, reinforced with bidirectional fibers is presented in finite plane elastostatics. The fiber's resistance to stretch and flexure are accounted for with variational computations of first and second gradient of deformations, respectively. Within the framework of strain-gradient elasticity, the Euler equation and necessary boundary conditions are formulated. A rigorous derivation of the corresponding linear theory is also developed from which, a complete analytical solution is obtained for small deformations superposed on large. In particular, we assimilate plane bias extension test results indicating that the proposed model successfully predicts smooth transitions of shear strain fields unlike those depicted by the first gradient theory where significant discontinuities are present. The proposed model can serve as an alternative 2D Cosserat theory of non-linear elasticity.

1. Introduction

Mechanics of materials with distinct microstructures have consistently been the subject of intense study (Pipkin, 1979; Spencer, 1972) due to their practical importance in materials science and engineering. It is widely believed that the microstructure of materials, in general, governs the overall mechanical responses (Hahm & Khang, 2010; Monecke, 1989; Moravec & Holecek, 2010; Voigt, 1887). Fiber-reinforced composites are a particular case of such materials where fibers, as the microstructure of the composite, are embedded in a matrix material. In practice, these fibers are often presumed to be densely distributed so as to render the idealization of continuous distribution which further leads to the continuum description of fiber-composites via a homogenization procedure. Within this setting, the composites can be regarded as a special type of anisotropic materials where the response function depends on the first gradient of deformations, typically augmented by the constraints of bulk compressibility or fiber inextensibility. In the latter case, the resulting prediction models are often so constrained that the corresponding deformation fields are essentially kinematically determinate, particularly that arise in fibers (Mulhern, Rogers, & Spencer, 1969; Pipkin & Rogers, 1971). Nonetheless, continuum-based approaches were used widely in the analysis of the mechanics of composite materials for their advantage in the continuum descriptions and the associated mathematical frame work (see, for example, (Mulhern, Rogers, & Spencer, 1967; 1969; Munch, Neff, & Wagner, 2011) and references therein).

The continuum theory, which accounts for the microstructural effects of fibers on elastic materials, has gained renewed attention in recent years (Spencer & Soldatos, 2007; Steigmann, 2012; Steigmann & dell'Isola, 2015). This includes the

* Corresponding author.
E-mail address: cikim@ualberta.ca (C.I. Kim).

https://doi.org/10.1016/j.ijengsci.2018.06.002
0020-7225/

"refinement" of the first-order continuum theory by considering the higher gradient of deformations in an effort to achieve a more detailed characterization of the continua with microstructures. In the case of fiber composites, this means the incorporation of the bending resistance of the fibers into the models of deformations. This is framed in the setting of the nonlinear strain-gradient theory (Koiter, 1964; Toupin, 1964; Truesdell & Noll, 1965) of anisotropic elasticity where the fibers' bending resistance is assigned to the changes in curvature (flexure) of fibers explicitly (Spencer & Soldatos, 2007). The latter is obtained via the computation of the second gradient of deformations in which the fibers are regarded as continuous curves, defined in convected coordinates. Current applications of the general theory are discussed in Maugin and Metrikine (2010); Munch et al. (2011); Neff (2006b); Park and Lakes (1987) , and mathematical aspects of the subject are presented in Fried and Gurtin (2009); Neff (2006a); Park and Gao (2008). A theory for an elastic solid with fiber's resistant to flexure, stretch and twist is developed in Steigmann (2012) under the simplified setting of the constraint Cosserat theory. In addition, authors in dell'Isola, Cuomo, Greco, and Della Corte (2017); dell'Isola, Della Corte, Greco, and Luongo (2016); Turco (2016) discussed second-gradient theory of elasticity for the mechanics of meshed structures and examined shear strain distributions of the meshed structure subjected to the plane bias extension. To this end, authors in Zeidi and Kim (2017a, 2017b, 2018) presented the continuum formulation of fiber-reinforced composites where the bending resistance of fibers is accounted for via the second gradient of deformations. However, the majority of the aforementioned studies were limited in scope, insofar as they considered either inextensible fibers or single family of fibers. Moreover, although recent studies (Cuomo, dell'Isola, & Greco, 2016; dell'Isola et al., 2017; dell'Isola et al., 2016; 2016) reveal that the second-gradient theory accurately predicts the smooth transitions of shear strain fields of meshed structures undergoing bias extensions, compatible results in the case of general fiber composites remain absent from the literature.

In the present work, we develop a continuum model which describes the mechanical responses of an elastic solid reinforced with bidirectional fibers and subjected to finite plane deformations. Thus, it is assumed that the fiber's directors remain in a plane, with no out-of-plane components and that the corresponding deformations and material parameters are independent of the out-of-plane coordinate. The bidirectional fibers are treated as continuously distributed spatial rods of Kirchhoff type such that the kinematics are defined by their position and director fields (Antman, 2005; Dill, 1992; Landau & Lifshitz, 1986). Within this prescription, we propose an energy functional that can accommodate fibers resistant to flexure and extension, and construct the constitutive relations by applying the variational principle on the first and second gradient of deformations, respectively. The corresponding Euler equilibrium equation is also derived by virtue of the virtual work statement. With the Euler equation satisfied, we present a rigorous derivation of the necessary boundary conditions in the case of bidirectional fibers. We then consider a special case of a Neo–Hookian material, reinforced with bidirectional fibers, and subsequently formulate systems of coupled Partial Differential Equations (PDEs) describing the deformations of fiber composites. The solutions of the resulting PDEs are obtained via the Finite Element Analysis (FEA), which demonstrate excellent correspondence with existing theoretical and experimental results (see, for example, (dell'Isola et al., 2017; dell'Isola et al., 2016; Dong & Davies, 2015)).

More importantly, the proposed model assimilates, in the case of bidirectional fiber composites, the plane bias extension test and successfully predicts the smooth transitions of the corresponding shear strain fields, as opposed to the first-gradient theory, where the resulting shear strain appears to be discontinued. In addition, we develop a compatible linear theory within the description of superposed incremental deformations (Ogden, 1984). By employing adapted iterative reduction and eigenfunction expansion methods (Huang & Zhang, 2002; Read, 1993; 1996), a complete analytical solution is obtained, which describes the responses of a bidirectional composite subjected to flexure and extension. The analytical solution is smooth and stable within the entire domain of interest and demonstrates good agreement with the experiment (Dong & Davies, 2015) and FEA results for small deformations superposed on large. Lastly, we note here that the proposed model can serve as an alternative 2D Cosserat theory of nonlinear elasticity (Pietraszkiewicz & Eremeyev, 2009; Reissner, 1987; Toupin, 1964; Truesdell & Noll, 1965).

Throughout the paper, we make use of a number of well-established symbols and conventions such as $\mathbf{A}^T$, $\mathbf{A}^{-1}$, $\mathbf{A}^*$ and $tr(\mathbf{A})$. These are the transpose, the inverse, the cofactor and the trace of a tensor $\mathbf{A}$, respectively. The tensor product of vectors is indicated by interposing the symbol $\otimes$, and the Euclidian inner product of tensors $\mathbf{A}$, $\mathbf{B}$ is defined by $\mathbf{A}\cdot\mathbf{B} = tr(\mathbf{A}\mathbf{B}^T)$; the associated norm is $|\mathbf{A}| = \sqrt{\mathbf{A}\cdot\mathbf{A}}$. The symbol $|*|$ is also used to denote the usual Euclidian norm of three-vectors. Latin and Greek indices take values in {1, 2} and, when repeated, are summed over their ranges. Lastly, the notation $F_{\mathbf{A}}$ stands for the tensor-valued derivatives of a scalar-valued function $F(\mathbf{A})$.

2. Kinematics and equilibrium equations

Let $\mathbf{L}$ and $\mathbf{M}$ be the unit tangent to the fiber's trajectory in the reference configuration and $\mathbf{l}$ and $\mathbf{m}$ are their counterparts in the deformed configuration. The orientations of particular bidirectional fibers are then given by

$$\lambda = |\eta| = \frac{ds}{dS},\ \ \mu = |\tau| = \frac{du}{dU} \text{ and } \mathbf{l} = \eta\lambda^{-1},\ \ \mathbf{m} = \tau\gamma^{-1}, \tag{1}$$

where

$$\mathbf{FL} = \lambda\mathbf{l} \text{ and } \mathbf{FM} = \gamma\mathbf{m}, \tag{2}$$

and $\mathbf{F}$ is the gradient of the deformation function ($\boldsymbol{\chi}(\mathbf{X})$). Eq. (2) can be derived by taking the derivative of $\mathbf{r}(s(S)) = \chi(\mathbf{X}(S))$, with respect to arclength parameters, S, and ultimately, s, upon making the identifications $\mathbf{L} = \frac{d\mathbf{X}}{dS}$ and $\mathbf{l} = \frac{d\chi}{ds}$ and similarly

for $\mathbf{M}$ (i.e. $\mathbf{M}=\frac{d\mathbf{X}}{dU}$ and $\mathbf{m}=\frac{d\chi}{du}$). Here, $\frac{d(*)}{dS}$, $\frac{d(*)}{dU}$ and $\frac{d(*)}{ds}$, $\frac{d(*)}{du}$ refer to the arclength derivatives of $(*)$ along the fibers' directions in the reference and deformed configurations, respectively. In the present study, we limit our attention to the case of initially orthogonal fibers:

$$\mathbf{M}\cdot\mathbf{L}=\mathbf{0}. \tag{3}$$

We note here that initially non-orthogonal fibers can be accommodated by setting $\mathbf{M}\cdot\mathbf{L}=\cos\delta$ (see, for example, (Steigmann & dell'Isola, 2015)) which is beyond the scope of this paper. Combining Eqs. (2) and (3) furnishes a useful fiber decomposition of the deformation gradient that

$$\mathbf{F}=\lambda\mathbf{l}\otimes\mathbf{L}+\gamma\mathbf{m}\otimes\mathbf{M}. \tag{4}$$

Therefore we have, for example, $\mathbf{L}=L_A\mathbf{E}_A$ and $\mathbf{l}=l_i\mathbf{e}_i$ to yield

$$\lambda l_i=F_{iA}L_A, \tag{5}$$

where $\{\mathbf{E}_A\},\{\mathbf{e}_i\}$ are orthonormal bases in the reference and deformed configurations. Further, the expressions for geodesic curvatures of a parametric curve $(\mathbf{r}(s,u))$ can be obtained from Eq. (2) that

$$\mathbf{g}_1=\frac{d^2\mathbf{r}(S)}{dS^2}=\frac{d(\frac{\mathbf{r}(S)}{dS})}{dS}=\frac{\partial(\mathbf{FL})}{\partial\mathbf{X}}\frac{d\mathbf{X}}{dS}=\nabla[\mathbf{FL}]\mathbf{L}, \tag{6}$$

and

$$\mathbf{g}_2=\frac{d^2\mathbf{r}(U)}{dU^2}=\frac{d(\frac{\mathbf{r}(U)}{dU})}{dU}=\frac{\partial(\mathbf{FM})}{\partial\mathbf{X}}\frac{d\mathbf{X}}{dU}=\nabla[\mathbf{FM}]\mathbf{M}. \tag{7}$$

In general, most of the fibers are straight prior to deformations. Even slightly curved fibers can be idealized as 'fairly straight' fibers, considering their length scales with respect to that of matrix materials. This suggests that the gradients of unit tangents in the reference configuration are vanishes identically (i.e. $\nabla\mathbf{L}=\nabla\mathbf{M}=\mathbf{0}$). Accordingly, Eqs. (6) and (7) become

$$\mathbf{g}_1=\nabla\mathbf{F}(\mathbf{L}\otimes\mathbf{L}) \text{ and } \mathbf{g}_2=\nabla\mathbf{F}(\mathbf{M}\otimes\mathbf{M}). \tag{8}$$

We now introduce the convention of the second gradient of deformations as

$$\nabla\mathbf{F}\equiv\mathbf{G}, \tag{9}$$

where the compatibility condition of $\mathbf{G}$ is given by

$$G_{iAB}=F_{iA,B}=F_{iB,A}=G_{iBA}. \tag{10}$$

Thus,

$$\mathbf{g}_1=\mathbf{G}(\mathbf{L}\otimes\mathbf{L})=\mathbf{g}_1(\mathbf{G}) \text{ and } \mathbf{g}_2=\mathbf{G}(\mathbf{M}\otimes\mathbf{M})=\mathbf{g}_2(\mathbf{G}). \tag{11}$$

The forgoing developments suggest that the mechanical responses of fiber-matrix systems can be described by the following energy function:

$$W(\mathbf{F},\mathbf{G})=\widehat{W}(\mathbf{F})+W(\mathbf{G}),\quad W(\mathbf{G})\equiv\frac{1}{2}C_1(\mathbf{F})|\mathbf{g}_1|^2+\frac{1}{2}C_2(\mathbf{F})|\mathbf{g}_2|^2, \tag{12}$$

where $C_i(\mathbf{F})$ refers to the material property of fibers which are, in general, independent of the deformation gradient (i.e. $C_i(\mathbf{F})=C_i$**).** Eq. (12) presumes that fiber's bending energy is solely accounted for by the second gradient of deformations, $\mathbf{G}$, as depicted in Eq. (11). This concept has been widely and successfully adopted in the relevant subjects of studies (see, for example, Spencer and Soldatos (2007) and Steigmann and dell'Isola (2015)). To accommodate fibers resistant to extension, we compute their strains as

$$\varepsilon_1=\frac{1}{2}\left(\lambda^2-1\right)=\frac{1}{2}[(\mathbf{F}^{\mathbf{T}}\mathbf{F})\cdot\mathbf{L}\otimes\mathbf{L}-1], \tag{13}$$

and

$$\varepsilon_2=\frac{1}{2}\left(\gamma^2-1\right)=\frac{1}{2}[(\mathbf{F}^{\mathbf{T}}\mathbf{F})\cdot\mathbf{M}\otimes\mathbf{M}-1], \tag{14}$$

where, the expressions of λ^2 and μ^2 are obtained from Eqs. (2) and (3) that

$$\lambda^2=\mathbf{FL}\cdot\mathbf{FL}=\mathbf{F}^T\mathbf{FL}\cdot\mathbf{L}=(\mathbf{F}^{\mathbf{T}}\mathbf{F})\cdot\mathbf{L}\otimes\mathbf{L}, \tag{15}$$

and similarly for

$$\gamma^2=(\mathbf{F}^{\mathbf{T}}\mathbf{F})\cdot\mathbf{M}\otimes\mathbf{M}. \tag{16}$$

It is clear from Eqs. (13) and (14) that the fibers' extensions are $\mathbf{F}$ dependent. Hence, $\widehat{W}(\mathbf{F})$ is required to be a function of strain parameters (i.e. ε_1 and ε) for extensible fibers as

$$\widehat{W}(\mathbf{F})=W(I,\ \varepsilon_1,\ \varepsilon_2), \tag{17}$$

where $I = tr\mathbf{C}$ and $\mathbf{C} = \mathbf{F}^{\mathbf{T}}\mathbf{F}$ is the right Cauchy–Green deformation tensor, which is also dependent on $\mathbf{F}$. Consequently, the response function (12) can be expressed in the following explicit form

$$\widehat{W}(\mathbf{F}) + W(\mathbf{G}) = W(I,\ \varepsilon_1,\ \varepsilon_2,\ \mathbf{g}_1,\ \mathbf{g}_2) = W(I,\ \varepsilon_1,\ \varepsilon_2) + \frac{1}{2}C_1|\mathbf{g}_1|^2 + \frac{1}{2}C_2|\mathbf{g}_2|^2. \tag{18}$$

For use in the Euler equations and natural boundary conditions, we evaluate the induced energy variation of the response function using chain rule,

$$\frac{\partial W}{\partial F_{iA}}\dot{F}_{iA} + \frac{\partial W}{\partial G_{iAB}}\dot{G}_{iAB} = \dot{W}. \tag{19}$$

In the above, the superposed dot refers to derivatives with respect to a parameter ε at a fixed value (e.g. $\varepsilon = 0$ at equilibrium) that labels a one-parameter family of deformations. Accordingly, from (18), we obtain

$$\dot{W} = \dot{W}(I,\ \varepsilon_1,\ \varepsilon_2,\ \mathbf{g}_1,\ \mathbf{g}_2) = W_I\dot{I} + W_{\varepsilon_1}\dot{\varepsilon}_1 + W_{\varepsilon_2}\dot{\varepsilon}_2 + W_{\mathbf{g}_1}\cdot\dot{\mathbf{g}}_1 + W_{\mathbf{g}_2}\cdot\dot{\mathbf{g}}_2, \tag{20}$$

in which we have used the fact that W depends on the deformation through I, ε_1, ε_2, $\mathbf{g}_1$, $\mathbf{g}_2$ and ultimately $\mathbf{F}$ and $\mathbf{G}$. The required expressions can be equated in terms of $\mathbf{F}$ such that

$$\dot{I} = [tr(\mathbf{C})\dot{]} = (\mathbf{I}\cdot\dot{\mathbf{C}}) = \mathbf{I}\cdot\dot{\mathbf{C}} = 2\mathbf{F}\cdot\dot{\mathbf{F}} \tag{21}$$

Further, Eq. (15) yields

$$\dot{\varepsilon}_1 = \dot{\lambda}\lambda = \mathbf{FL}\cdot\dot{\mathbf{FL}} = tr(\mathbf{FL}\otimes\dot{\mathbf{FL}}) = tr((\mathbf{FL}\otimes\mathbf{L})\dot{\mathbf{F}}^T) = \mathbf{FL}\otimes\mathbf{L}\cdot\dot{\mathbf{F}}. \tag{22}$$

and similarly for

$$\dot{\varepsilon}_2 = \dot{\gamma}\gamma = \mathbf{FM}\otimes\mathbf{M}\cdot\dot{\mathbf{F}}. \tag{23}$$

In particular, the variational derivative with respect to the second gradient of deformations is equivalent to (see, Eq. (12))

$$\dot{W}(\mathbf{G}) = W_{\mathbf{G}}\cdot\dot{\mathbf{G}} = C_1\mathbf{g}_1\cdot\dot{\mathbf{g}}_1 + C_2\mathbf{g}_2\cdot\dot{\mathbf{g}}_2, \tag{24}$$

where, in the case of initially straight fibers (i.e. $\dot{\mathbf{L}} = \dot{\mathbf{M}} = \mathbf{0}$), from Eq. (11), $\dot{\mathbf{g}}_1 = \dot{\mathbf{G}}(\mathbf{L}\otimes\mathbf{L})$ and $\dot{\mathbf{g}}_2 = \dot{\mathbf{G}}(\mathbf{M}\otimes\mathbf{M})$. Therefore, the above can be rewritten as

$$W_{\mathbf{G}}\cdot\dot{\mathbf{G}} = \dot{\mathbf{G}}\cdot(C_1\mathbf{g}_1\otimes\mathbf{L}\otimes\mathbf{L} + C_2\mathbf{g}_2\otimes\mathbf{M}\otimes\mathbf{M}). \tag{25}$$

Finally, by comparing both sides of Eq. (25), we derive

$$\frac{\partial W}{\partial G_{iAB}} = C_1(g_1)_i L_A L_B + C_2(g_2)_i M_A M_B. \tag{26}$$

The constraint of bulk incompressibility can be accommodated via the following form of an augmented energy potential:

$$U(I,\ \varepsilon_1,\ \varepsilon_2,\ \mathbf{g}_1,\ \mathbf{g}_2) = W(I,\ \varepsilon_1,\ \varepsilon_2,\ \mathbf{g}_1,\ \mathbf{g}_2) - p(J-1), \tag{27}$$

where J is determinant of $\mathbf{F}$ and p is a Lagrange-multiplier field. Since $\dot{J} = \frac{\partial J}{\partial \mathbf{F}}\cdot\dot{\mathbf{F}} = J\left(\mathbf{F}^{-1}\right)^T\cdot\dot{\mathbf{F}} = \mathbf{F}^*\cdot\dot{\mathbf{F}}$, Eqs. (21), (23) and (27) furnish

$$\dot{U} = 2W_I\mathbf{F}\cdot\dot{\mathbf{F}} + W_{\varepsilon_1}\mathbf{FL}\otimes\mathbf{L}\cdot\dot{\mathbf{F}} + W_{\varepsilon_2}\mathbf{FM}\otimes\mathbf{M}\cdot\dot{\mathbf{F}} - p\mathbf{F}^*\cdot\dot{\mathbf{F}} + C_1\mathbf{g}_1\cdot\dot{\mathbf{g}}_1 + C_2\mathbf{g}_2\cdot\dot{\mathbf{g}}_2. \tag{28}$$

But from (24) and (25), the above reduces to

$$\dot{U} = (2W_I\mathbf{F} + W_{\varepsilon_1}\mathbf{FL}\otimes\mathbf{L} + W_{\varepsilon_2}\mathbf{FM}\otimes\mathbf{M} - p\mathbf{F}^*)\cdot\dot{\mathbf{F}} + W_{\mathbf{G}}\cdot\dot{\mathbf{G}}, \tag{29}$$

or, equivalently,

$$\dot{U} = (2W_I F_{iA} + W_{\varepsilon_1}F_{iB}L_A L_B + W_{\varepsilon_2}F_{iB}M_A M_B - pF^*_{iA})\dot{F}_{iA} + \frac{\partial W}{\partial G_{iAB}}\dot{G}_{iAB}.$$

Eq. (29) reflects the fact that the mechanical responses of the matrix material and fibers' stretch are associated with the first gradient, $\mathbf{F}$, albeit the bending resistance of the fibers is accommodated by the second gradient, $\mathbf{G}$ (see, also, Spencer & Soldatos (2007)).

3. Equilibrium

The derivation of the Euler equation and boundary conditions arising in second-gradient elasticity are well studied (Germain, 1973; Koiter, 1964; Mindlin & Tiersten, 1962; Toupin, 1964). We reformulate the results in the present context for the sake of clarity and completeness. The weak form of the equilibrium equations is given by the virtual-work statement,

$$\dot{E} = P, \tag{30}$$

where the superposed dot refers to the variational and/or Gateâux derivative,

$$E = \int_\Omega U(\mathbf{F}, \mathbf{G}) dA \tag{31}$$

is the strain energy and P is the virtual power of the applied loads. In the above, the conservative loads are characterized by the existence of a potential L such that $P = \dot{L}$. Therefore, the problem of determining equilibrium deformations is reduced, in the present case, to the problem of minimizing the potential energy, $E - L$. Accordingly, we have

$$\dot{E} = \int_\Omega \dot{U}(\mathbf{F}, \mathbf{G}) dA, \tag{32}$$

where the expression of $\dot{U}$ is given by (29). From Eq. (10), the energy variation with respect to the second gradient of deformations (i.e. $\dot{W}(\mathbf{G}) = W_{\mathbf{G}} \cdot \dot{\mathbf{G}}$) can be rewritten as

$$W_{\mathbf{G}} \cdot \dot{\mathbf{G}} = \frac{\partial W}{\partial G_{iAB}} \dot{G}_{iAB} = \frac{\partial W}{\partial G_{iAB}} \dot{F}_{iA,B} = \frac{\partial W}{\partial G_{iAB}} u_{i,AB}, \tag{33}$$

and

$$\frac{\partial W}{\partial G_{iAB}} u_{i,AB} = \left(\frac{\partial W}{\partial G_{iAB}} u_{i,A} \right)_{,B} - \left(\frac{\partial W}{\partial G_{iAB}} \right)_{,B} u_{i,A}, \tag{34}$$

where $u_i = \dot{\chi}_i$ is the variation of the position field. Substituting Eqs. (29) and (34) into the Eq. (32) yields

$$\dot{E} = \int_\Omega [(2W_I F_{iA} + W_{\varepsilon_1} F_{iB} L_A L_B + W_{\varepsilon_2} F_{iB} M_A M_B - p F^*_{iA}) u_{i,A} + \left(\frac{\partial W}{\partial G_{iAB}} u_{i,A} \right)_{,B} - \left(\frac{\partial W}{\partial G_{iAB}} \right)_{,B} u_{i,A}] dA. \tag{35}$$

Thus, we obtain

$$\dot{E} = \int_\Omega [2W_I F_{iA} + W_{\varepsilon_1} F_{iB} L_A L_B + W_{\varepsilon_2} F_{iB} M_A M_B - p F^*_{iA} - \left(\frac{\partial W}{\partial G_{iAB}} \right)_{,B}] u_{i,A} dA + \int_{\partial\Omega} \frac{\partial W}{\partial G_{iAB}} u_{i,A} N_B dS, \tag{36}$$

where $\mathbf{N}$ is the rightward unit normal to $\partial\Omega$ in the sense of Green–Stokes theorem. Further, for initially straight fibers (i.e. $\dot{\mathbf{L}} = \dot{\mathbf{M}} = \mathbf{0}$), $Div(W_{\mathbf{G}})$ reduces to

$$\begin{aligned} Div(W_{\mathbf{G}}) &= C_1 (g_1)_{i,B} L_A L_B (\mathbf{e}_i \otimes \mathbf{E}_A) + C_2 (g_2)_{i,B} M_A M_B (\mathbf{e}_i \otimes \mathbf{E}_A) \\ &= [C_1 (g_1)_{i,B} L_A L_B + C_2 g^2_{i,B} M_A M_B] (\mathbf{e}_i \otimes \mathbf{E}_A), \\ &\because \left(\frac{\partial W}{\partial G_{iAB}} \right)_{,B} = C_1 (g_1)_{i,B} L_A L_B + C_2 g^2_{i,B} M_A M_B. \end{aligned} \tag{37}$$

Consequently, Eq. 36 furnishes

$$\dot{E} = \int_\Omega P_{iA} \dot{F}_{iA} dA + \int_{\partial\Omega} \frac{\partial W}{\partial G_{iAB}} \dot{F}_{iA} N_B dS, \tag{38}$$

where

$$P_{iA} = 2W_I F_{iA} + W_{\varepsilon_1} F_{iB} L_A L_B + W_{\varepsilon_2} F_{iB} M_A M_B - p F^*_{iA} - C_1 (g_1)_{i,B} L_A L_B - C_2 (g_2)_{i,B} M_A M_B, \tag{39}$$

and hence the Euler equation is obtained by

$$P_{iA,A} = 0 \text{ or } Div(\mathbf{P}) = 0 \tag{40}$$

which holds in Ω.

3.1. Example: Neo–Hookean type materials

In the case of incompressible neoHookean-type materials, the energy density function is given by

$$W^1(I) = \mu(I-3), \tag{41}$$

Further, in order to accommodate fiber's resistance to extension, we propose the following augmented energy potential of quadratic form

$$W^2(\varepsilon_1,\ \varepsilon_2) = E_1\frac{1}{2}\varepsilon_1^2 + E_2\frac{1}{2}\varepsilon_2^2, \tag{42}$$

where E_i are the elastic modulus of fibers (extension). Combining Eqs. (41) and (42) yields

$$W(I,\ \varepsilon_1,\ \varepsilon_2) = W^1(I) + W^2(\varepsilon_1,\ \varepsilon_2) = \mu(I-3) + E_1\frac{1}{2}\varepsilon_1^2 + E_2\frac{1}{2}\varepsilon_2^2. \tag{43}$$

We now substitute the above into Eq. (18) and thereby obtain

$$W(I,\ \varepsilon_1,\ \varepsilon_2,\ \mathbf{g}_1,\ \mathbf{g}_2) = W(I,\ \varepsilon_1,\ \varepsilon_2) + W(\mathbf{G}) = \mu(I-3) + \frac{1}{2}E_1\varepsilon_1^2 + \frac{1}{2}E_2\varepsilon_2^2 + \frac{1}{2}C_1|\mathbf{g}_1|^2 + \frac{1}{2}C_2|\mathbf{g}_2|^2, \tag{44}$$

where μ and C_i are the material constant of the matrix and fibers (flexure), respectively. Also, the required expressions are computed via Eqs. (13), (14) and (41), so that

$$W_I = \mu,\ W_{\varepsilon_1} = E_1\varepsilon_1 = \frac{1}{2}E_1(\mathbf{FL}\cdot\mathbf{FL}-1) \text{ and } W_{\varepsilon_2} = E_2\varepsilon_2 = \frac{1}{2}E_2(\mathbf{FM}\cdot\mathbf{FM}-1). \tag{45}$$

Thus, Eq. (39) becomes

$$\begin{aligned} P_{iA} &= 2\mu F_{iA} + \frac{E_1}{2}(F_{jC}F_{jD}L_CL_D - 1)F_{iB}L_AL_B + \frac{E_2}{2}(F_{jC}F_{jD}M_CM_D - 1)F_{iB}M_AM_B \\ &\quad - pF^*_{iA} - C_1(g_1)_{i,B}L_AL_B - C_2(g_2)_{i,B}M_AM_B, \end{aligned} \tag{46}$$

and the corresponding Euler equation is formulated as

$$\begin{aligned} P_{iA,A} = 0 &= 2\mu F_{iA,A} - pF^*_{iA} + \frac{E_1}{2}(F_{iB,A}F_{jC}F_{jD} + F_{iB}F_{jC,A}F_{jD} + F_{iB}F_{jC}F_{jD,A})L_AL_BL_CL_D \\ &\quad + \frac{E_2}{2}(F_{iB,A}F_{jC}F_{jD} + F_{iB}F_{jC,A}F_{jD} + F_{iB}F_{jC}F_{jD,A})M_AM_BM_CM_D \\ &\quad - \frac{E_1}{2}F_{iB,A}L_AL_B - \frac{E_2}{2}F_{iB,A}M_AM_B - C_1(g_1)_{i,AB}L_AL_B - C_2(g_2)_{i,AB}M_AM_B, \end{aligned} \tag{47}$$

where $F^*_{iA,A} = 0$ (Piola's identity).

Let us now consider a fiber-reinforced material that consists of initially an orthonormal set of fibers,

$$\mathbf{L} = \mathbf{E}_1,\ L_1 = 1,\ L_2 = 0,\ \mathbf{M} = \mathbf{E}_2,\ M_1 = 0,\ M_2 = 1, \tag{48}$$

and is subjected to finite plane deformations. Accordingly, Eq. (47) reduces to

$$\begin{aligned} P_{iA,A} = 0 &= 2\mu F_{iA,A} - pF^*_{iA} + \frac{E_1}{2}(F_{i1,1}F_{j1}F_{j1} + F_{i1}F_{j1,1}F_{j1} + F_{i1}F_{j1}F_{j1,1}) \\ &\quad + \frac{E_2}{2}(F_{i2,2}F_{j2}F_{j2} + F_{i2}F_{j2,2}F_{j2} + F_{i2}F_{j2}F_{j2,2}) \\ &\quad - \frac{E_1}{2}F_{i1,1} - \frac{E_2}{2}F_{i2,2} - C_1(g_1)_{i,11} - C_2(g_2)_{i,22}, \end{aligned} \tag{49}$$

where

$$(g_1)_i = F_{i1,1},\ (g_2)_i = F_{i2,2},\ F_{iA} = \frac{\partial\chi_i}{\partial X_A},\ F^*_{iA} = \varepsilon_{ij}\varepsilon_{AB}F_{jB}, \tag{50}$$

and ε_{ij} is the 2-D permutation, $\varepsilon_{12} = -\varepsilon_{21} = 1, \varepsilon_{11} = -\varepsilon_{22} = 0$. Consequently, from Eqs. (49) and (50) together with the constraint of the bulk incompressibility ($\det\mathbf{F} = 1$), we obtain the following coupled PDE system, solving for χ_1, χ_2 and p as

$$\begin{aligned} 0 &= 2\mu(\chi_{1,11} + \chi_{1,22}) - p_{,1}\chi_{2,2} + p_{,2}\chi_{2,1} - \frac{E_1}{2}\chi_{1,11} - \frac{E_2}{2}\chi_{1,22} \\ &\quad + \frac{E_1}{2}(3\chi_{1,11}\chi_{1,1}\chi_{1,1} + \chi_{1,11}\chi_{2,1}\chi_{2,1} + 2\chi_{2,11}\chi_{1,1}\chi_{2,1}) \\ &\quad + \frac{E_2}{2}(3\chi_{1,22}\chi_{1,2}\chi_{1,2} + \chi_{1,22}\chi_{2,2}\chi_{2,2} + 2\chi_{2,22}\chi_{1,2}\chi_{2,2}) - C_1\chi_{1,1111} - C_2\chi_{1,2222} \\ 0 &= 2\mu(\chi_{2,11} + \chi_{2,22}) + p_{,1}\chi_{1,2} - p_{,2}\chi_{1,1} - \frac{E_1}{2}\chi_{2,11} - \frac{E_2}{2}\chi_{2,22} \end{aligned}$$

$$+\frac{E_1}{2}(3\chi_{2,11}\chi_{2,1}\chi_{2,1}+\chi_{2,11}\chi_{1,1}\chi_{1,1}+2\chi_{1,11}\chi_{1,1}\chi_{2,1})$$
$$+\frac{E_2}{2}(3\chi_{2,22}\chi_{2,2}\chi_{2,2}+\chi_{2,22}\chi_{1,2}\chi_{1,2}+2\chi_{1,22}\chi_{1,2}\chi_{2,2})-C_1\chi_{2,1111}-C_2\chi_{2,2222}$$
$$1=\chi_{1,1}\chi_{2,2}-\chi_{1,2}\chi_{2,1}. \tag{51}$$

4. Boundary conditions

Writing $P_{iA}u_{i,A}=(P_{iA}u_i)_{,A}-P_{iA,A}u_i$, we have from Eq. (38) that

$$\dot{E}=\int_{\partial\Omega}P_{iA}u_iN_AdS-\int_{\Omega}P_{iA,A}u_idA+\int_{\partial\Omega}\left(\frac{\partial W}{\partial G_{iAB}}u_{i,A}\right)N_BdS, \tag{52}$$

where the Green-Stoke's theorem is applied in the first term of Eq. (52). Since the Euler equation, $P_{iA,A}=0$ holds in Ω, the above reduces to

$$\dot{E}=\int_{\partial\Omega}P_{iA}u_iN_AdS+\int_{\partial\Omega}\left(\frac{\partial W}{\partial G_{iAB}}u_{i,A}\right)N_BdS. \tag{53}$$

In addition, $\nabla\mathbf{u}$ can be projected onto normal and tangential directions as

$$\nabla\mathbf{u}=\nabla\mathbf{u}(\mathbf{T}\otimes\mathbf{T})+\nabla\mathbf{u}(\mathbf{N}\otimes\mathbf{N})=\mathbf{u}'\otimes\mathbf{T}+\mathbf{u}_{,\mathbf{N}}\otimes\mathbf{N}, \tag{54}$$

where $\mathbf{u}'$ and $\mathbf{u}_{,N}$ are the tangential and normal derivatives of $\mathbf{u}$ on $\partial\Omega$ (i.e. $u_i'=u_{i,A}T_A,\ u_{i,N}=u_{i,A}N_A$) and $\mathbf{T}=\mathbf{X}'(S)=\mathbf{k}\times\mathbf{N}$ is the unit tangent to $\partial\Omega$, respectively. Hence Eq. (53) becomes

$$\dot{E}=\int_{\partial\Omega}P_{iA}u_iN_AdS+\int_{\partial\Omega}\frac{\partial W}{\partial G_{iAB}}\left(u_i'T_AN_B+u_{i,N}N_AN_B\right)dS. \tag{55}$$

By decomposing the second term of Eq. (55) as in Eq. (34), we obtain

$$\frac{\partial W}{\partial G_{iAB}}T_AN_Bu_i'=\left(\frac{\partial W}{\partial G_{iAB}}T_AN_Bu_i\right)'-\left(\frac{\partial W}{\partial G_{iAB}}T_AN_B\right)'u_i, \tag{56}$$

and therefore,

$$\dot{E}=\int_{\partial\Omega}\left[P_{iA}N_A-\left(\frac{\partial W}{\partial G_{iAB}}T_AN_B\right)'\right]u_idS+\int_{\partial\Omega}\frac{\partial W}{\partial G_{iAB}}u_{i,N}N_AN_BdS+\int_{\partial\Omega}\left(\frac{\partial W}{\partial G_{iAB}}T_AN_Bu_i\right)'dS. \tag{57}$$

From Eq. (25) (i.e. $\frac{\partial W}{\partial G_{iAB}}=C_1(g_1)_iL_AL_B+C_2(g_2)_iM_AM_B$), Eq. (57) can be rewritten as

$$\dot{E}=\int_{\partial\Omega}\left[P_{iA}N_A-\left(C_1g_i^1L_AT_AL_BN_B+C_2g_i^2M_AT_AM_BN_B\right)'\right]u_idS$$
$$+\int_{\partial\Omega}(C_1(g_1)_iL_AN_AL_BN_B+C_2(g_2)_iM_AN_AM_BN_B)u_{i,N}dS$$
$$-\sum\|(C_1(g_1)_iL_AT_AL_BN_B+C_2(g_2)_iM_AT_AM_BN_B)u_i\|, \tag{58}$$

where the double bar symbol refers to the jump across the discontinuities on the boundary, $\partial\Omega$ (i.e. $\|*\|=(*)^+-(*)^-$), and the sum refers to the collection of all discontinuities. It is concluded from (30) that admissible powers are of the form

$$P=\int_{\partial w_t}t_iu_idS+\int_{\partial w}m_iu_{i,N}dS+\sum f_iu_i. \tag{59}$$

Therefore, by comparing (58) and (59), we obtain

$$t_i=P_{iA}N_A-\frac{d}{dS}[C_1(g_1)_iL_AT_AL_BN_B+C_2(g_2)_iM_AT_AM_BN_B],$$
$$m_i=C_1(g_1)_iL_AN_AL_BN_B+C_2(g_2)_iM_AN_AM_BN_B,$$
$$f_i=C_1(g_1)_iL_AT_AL_BN_B+C_2(g_2)_iM_AT_AM_BN_B, \tag{60}$$

which are the expressions of edge tractions, edge moments and corner forces, respectively. For example, if the fiber's directions are either normal or tangential to the boundary (i.e. $(\mathbf{L}\cdot\mathbf{T})(\mathbf{L}\cdot\mathbf{N})=0$ and $(\mathbf{M}\cdot\mathbf{T})(\mathbf{M}\cdot\mathbf{N})=0$), (60) further reduces to

$$t_i=P_{iA}N_A,$$
$$m_i=C_1(g_1)_iL_AN_AL_BN_B+C_2(g_2)_iM_AN_AM_BN_B,$$
$$f_i=0, \tag{61}$$

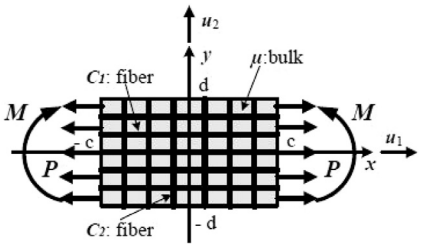

Fig. 1. Schematic of problem.

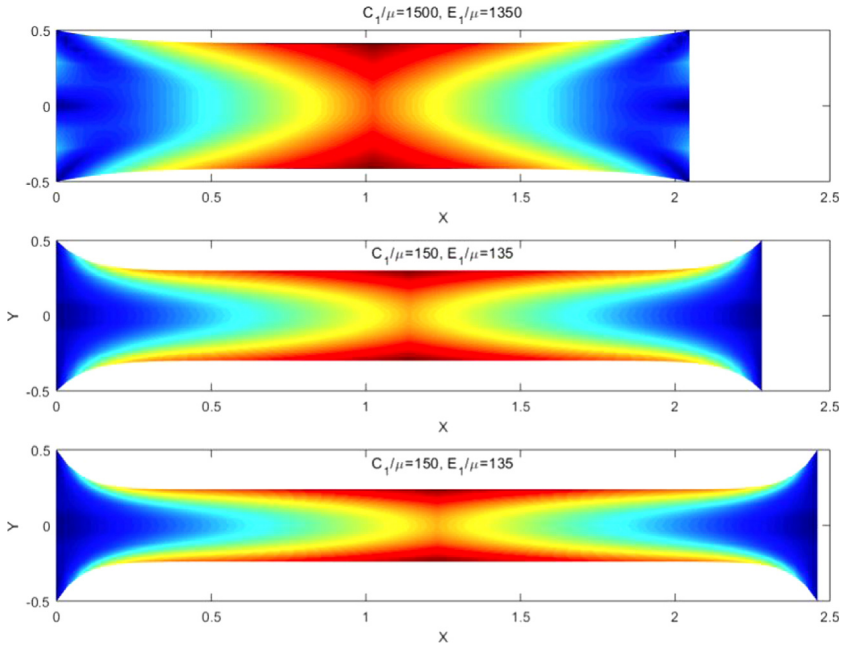

Fig. 2. Deformation contour $(\sqrt{\chi_1^2+\chi_2^2})$ with respect to C_1/μ, when $P_{11}/\mu = 50$, $C_2/\mu = 150$ and E_2/μ =135.

where

$$P_{iA} = 2W_I F_{iA} + W_{\varepsilon_1} F_{iB} L_A L_B + W_{\varepsilon_2} F_{iB} M_A M_B - pF^*_{iA} - C_1 (g_1)_{i,B} L_A L_B - C_2 (g_2)_{i,B} M_A M_B,$$
$$(g_1)_i = F_{iA,B} L_A L_B \text{ and } (g_2)_i = F_{iA,B} M_A M_B. \tag{62}$$

Finally, by imposing the admissible boundary conditions, (Eq. 61), solutions of the PDE system (Eq. 51) can be obtained via commercial packages (e.g. Matlab, COMSOL etc...). For the sake of coherence, details regarding Finite Element Analysis (FEA) formulations are reserved in the appendix. In the simulations, we consider the case where an elastic solid is reinforced with bidirectional fibers and subjected to finite plane deformations (either axial stretch or bending is considered), as illustrated in Fig. 1. It is also noted here that data are obtained under the normalized setting (e.g. $\frac{C_1}{\mu} = 150$, $\frac{E_1}{\mu} = 100$, $\frac{M}{\mu} = 5[L]^3$, etc...).

Figs. 2–4 illustrate the fiber composite's deformations under the axial tension. From Eqs. (46) and (61), the expression of the applied load P_{11} is obtained as

$$P_{11} = 2\mu\chi_{1,1} + \frac{E_1}{2}(\chi_{1,1}\chi_{1,1} + \chi_{2,1}\chi_{2,1} - 1)\chi_{1,1} - p\chi_{2,2} - C_1\chi_{1,111}. \tag{63}$$

It is clear from Figs. 2–4 that the axial extension is sensitive to the fibers' elastic resistance along the lateral direction. More precisely, the net amount of axial extension decreases with increasing values of C_1, E_1, C_2 and E_2. In particular, we assimilate the plane bias extension test in order to examine the effects of second-gradients of deformations onto the shear responses of the bidirectional fiber composites. The corresponding shear strains are computed via the relation $\phi' = \frac{u_2''(1+u_1') - u_2' u_1''}{u_2'^2 + (1+u_1')^2}$, where ϕ' is the rate of shear angle change. (see, (Dell'Isola, Giorgio, Pawlikowski, & Rizzi, 2016)). The results in Figs. 3 and 4 clearly indicate that the proposed model successfully predicts the smooth transitions of the shear strain fields, unlike those described by the first-order theory where a significant discontinuity is present (Fig. 5: left). The compatible results,

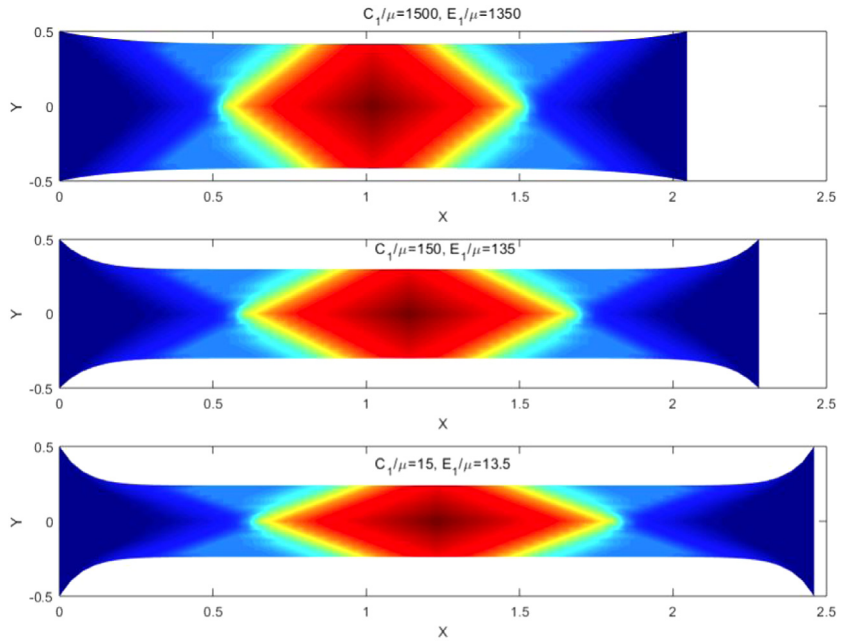

Fig. 3. Shear strain contour with respect to C_1/μ when $P_{11}/\mu = 50$, $C_2/\mu = 150$ and E_2/μ =135.

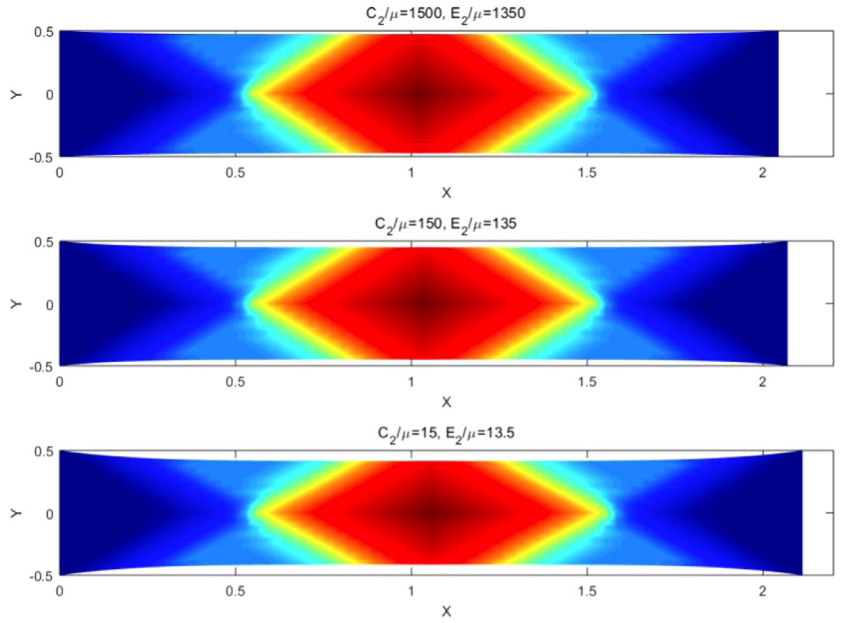

Fig. 4. Shear strain contour with respect to C_2/μ when $P_{11}/\mu = 50$, $C_1/\mu = 1500$ and E_2/μ =1350.

in cases of meshed structures, can be found in the work of dell'Isola et al. (2017, 2016), which also demonstrate a close agreement with the presented results (see, for example, Fig. 14 in dell'Isola et al. (2016)).

In order to examine fibers' reinforcing effects against to flexure, we also consider a rectangular fiber composite where one end is fixed and the other end is subjected to constant bending moment. The corresponding boundary conditions are imposed as, $\chi_{1,11} = -M/\mu$, $\chi_{2,11} = 0$, $\chi_2 = 0$ and $\chi_1 = 0$ at $x = 0$, and $\chi_{1,11} = -M/\mu$, $\chi_{2,11} = 0$, $\chi_{2,1} = 0$ and $\chi_{1,1} = 0$ at $x = c$. For the upper $(y = d)$ and bottom $(y = -d)$ faces, compatible boundary conditions are prescribed where we impose zero moment (i.e. $\chi_{2,22} = 0$ on the designated boundary). The resulting deformed profiles and contours demonstrate smooth transitions as they approach the boundary (see, Figs. 6 and 7). Further, Fig. 6 illustrates that the magnitude of deformation decreases as the fiber's bending stiffness increases.

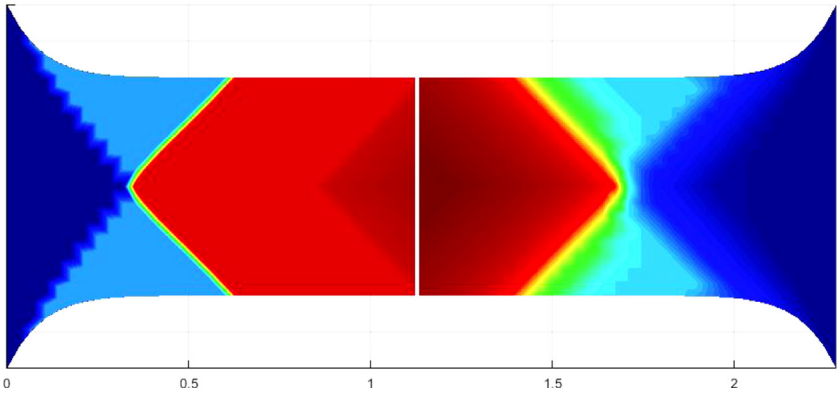

Fig. 5. Shear strain contour: 1st gradient (left) VS 2rd gradient (right).

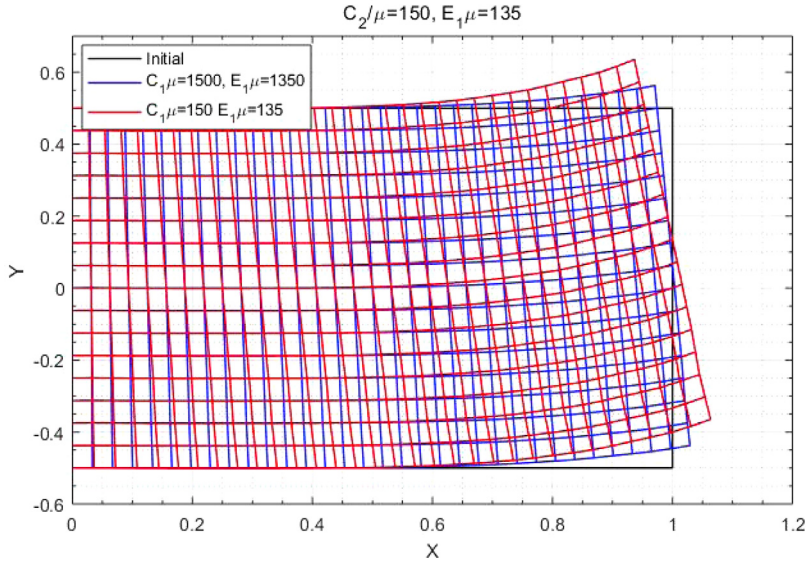

Fig. 6. Deformed configurations with respect to C_1/μ when M/μ =80.

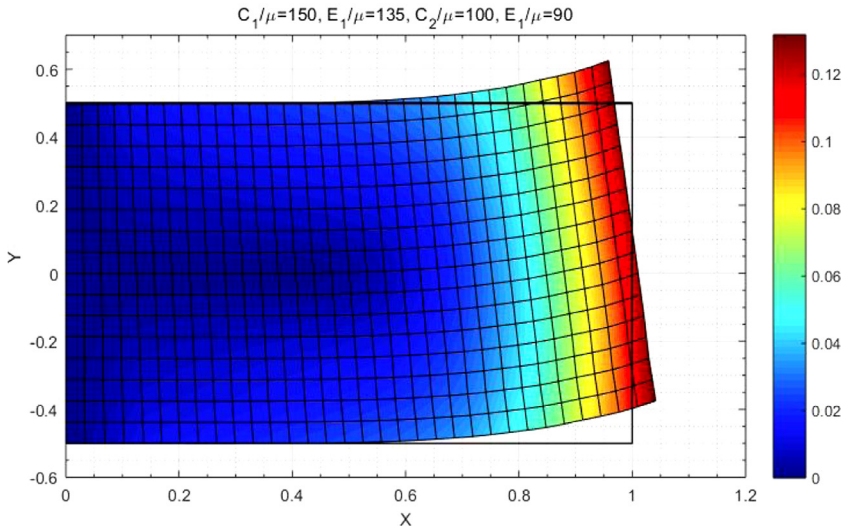

Fig. 7. Deformation contour ($\sqrt{\chi_1^2+\chi_2^2}$) when $M/\mu = 60$.

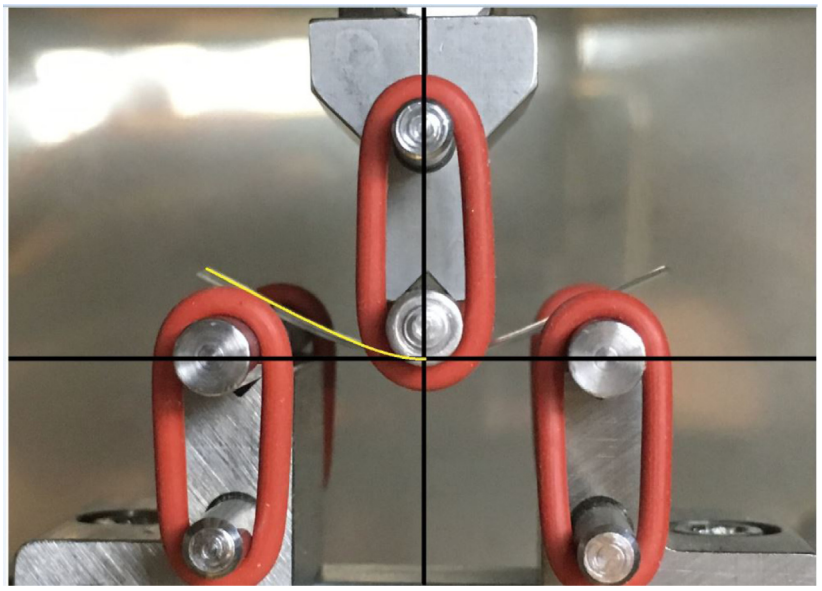

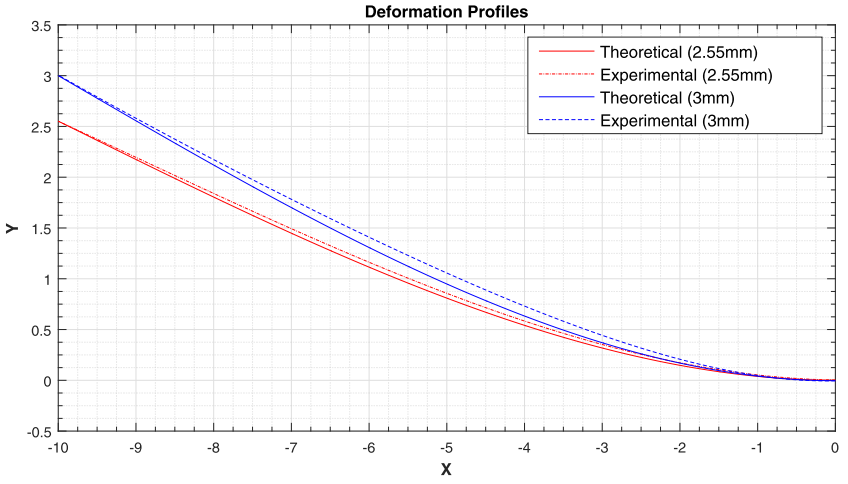

Fig. 8. CNC fiber composite bending test (2.55 mm and 3 mm) and theoretical predictions.

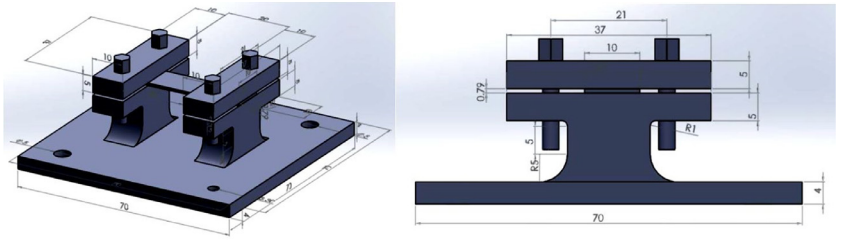

Fig. 9. Experimental setting: nylon-6 fiber neoprene rubber composite.

Comparisons with experimental results are successively performed to determine the accuracy and utility of the proposed model. Three sets of experiments are designed for the purpose: two from inhouse experimental settings and the other from the work of Dong. For the inhouse experiments, we considered a 3 point bending test of a crystalline nanocellulose (CNC) fiber composite ($C_1 = 150GPa, E_1 = 135GPa,\ \mu = 1GPa$), and an impact bending test of a Nylon-6 Fiber Neoprene Rubber Composite ($C_1 = 2000Mpa,\ E_1 = 1300Mpa,\ \mu = 2Mpa$). In the tests, the out-of-plane direction (x_3) is aligned with the loading cylinder and/or line of impact (see, Figs. 8 and 9). These are special cases of the proposed model, when $c \gg d$with

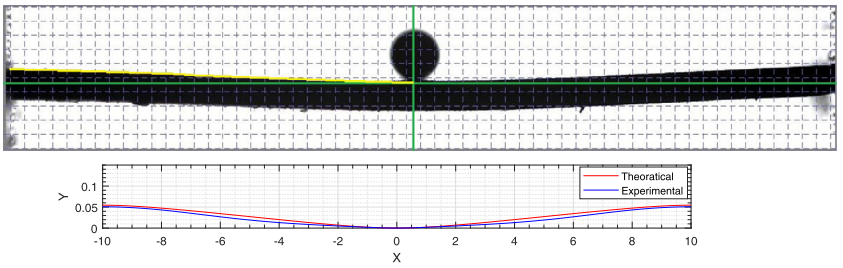

Fig. 10. Deformation profiles: theoretical predictions VS experimental results.

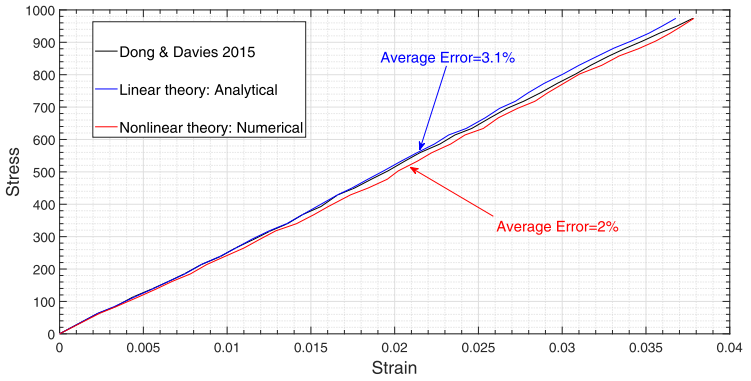

Fig. 11. Strain-stress curve: carbon-glass fiber composite.

vanishing C_2/μ and E_2/μ (see, Fig. 9). The solutions from our model successfully predict the deformations of both the CNC composites and the Nylon-6 Fiber Neoprene Rubber Composite with a maximum error of less than 3% (Figs. 8 –10.

In regard to the bending test of the bidirectional fiber composite reinforced with E glass and T700S carbon fibers (C_1 = carbon $= 4900MPa$, C_2 = glass $= 2240MPa$), we took the experimental results from the work of Dong and Davies (Dong and Davies (2015); Fig. 2 and Table 2). It is clear from Fig. 11 that predictions from the proposed model demonstrate a close agreement with the experimental data. Further, it is noted here that the compatible linear model, which is developed in the following section, also produces reasonably accurate result (See, Fig. 11; Linear theory: Analytical.).

The above results, in turn, suggest that the proposed model accurately describes the fiber's elastic resistance to flexures and extension through the first and second gradients of deformations. Lastly, we mention that the obtained solution accommodates the results from Zeidi and Kim (2017b) in the limit of vanishing fibers elastic resistance in y direction (i.e $C_2 = 0,\ E_2 = 0$) (See, Fig. 12).

5. Linear theory

We prescribe superposed "*small*" deformations as

$$\chi = \chi_o + \epsilon\dot{\chi}\ ; |\epsilon| \ll 1, \tag{64}$$

where $(^*)_o$ refers to the configuration of * evaluated at $\epsilon = 0$ and $(\dot{*}) = \partial(*)/\partial\varepsilon$. In particular, we denote $\dot{\chi} = \mathbf{u}$ in the forthcoming derivations, where applicable. Here caution needs to be taken that the present notation is not confused with the one used for the variational computation. From Eq. (64), the deformation gradient tensor is obtained by

$$\mathbf{F} = \mathbf{F}_o + \epsilon\nabla\mathbf{u}, \ \text{ where } \dot{\mathbf{F}} = \nabla\mathbf{u}. \tag{65}$$

In the analysis, we assume that the body is initially undeformed and stress free (i.e. at $\varepsilon = 0$, $\mathbf{F}_o = \mathbf{I}$ and $\mathbf{P}_o = \mathbf{0}$). Hence, Eq. (65) becomes

$$\mathbf{F} = \mathbf{I} + \epsilon\nabla\mathbf{u}, \tag{66}$$

and successively yields

$$\mathbf{F}^{-1} = \mathbf{I} - \epsilon\nabla\mathbf{u} + o(\epsilon) \text{ and } J = \det\mathbf{F} = 1 + \epsilon\,\mathrm{div}\,\mathbf{u} + o(\epsilon). \tag{67}$$

Further, in view of Eq. (64), Eq. (40) can be approximated as

$$Div(\mathbf{P}) = Div(\mathbf{P}_o) + \epsilon Div(\dot{\mathbf{P}}) + o(\epsilon) = \mathbf{0}. \tag{68}$$

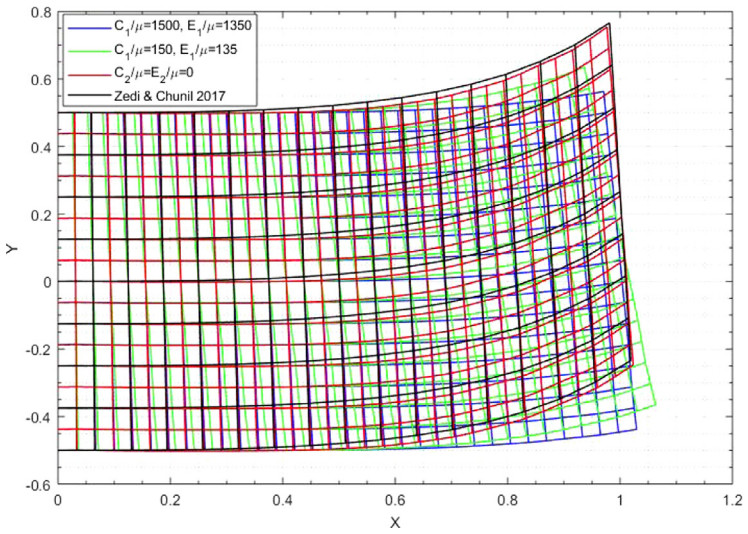

Fig. 12. Deformation profiles: proposed model VS *Zeidi* & *Chunil.* 2017.

Dividing the above by ϵ and letting $\epsilon \to 0$, we find

$$Div(\dot{\mathbf{P}}) = 0 \text{ or } \dot{P}_{iA,A} = 0, \tag{69}$$

which serves as the compatible linearized Euler equation. Now, from Eq. (39), the induced variation of $\mathbf{P}$ with respect to ϵ can be evaluated as

$$\begin{aligned}\dot{P}_{iA} &= 2(W_{II}\dot{I} + W_{I\varepsilon_1}\dot{\varepsilon}_1 + W_{I\varepsilon_2}\dot{\varepsilon}_2)(F_{iA})_o + 2(W_I)_o\dot{F}_{iA} - \dot{p}(F^*_{iA})_o - p_o\dot{F}^*_{iA}\\ &+[(W_{I\varepsilon_1}\dot{I} + W_{\varepsilon_1\varepsilon_1}\dot{\varepsilon}_1 + W_{\varepsilon_1\varepsilon_2}\dot{\varepsilon}_2)(F_{iB})_o + (W_{\varepsilon_1})_o\dot{F}_{iB} - C_1(\dot{g}_1)_{i,B}]L_AL_B\\ &+[(W_{I\varepsilon_2}\dot{I} + W_{\varepsilon_1\varepsilon_2}\dot{\varepsilon}_1 + W_{\varepsilon_2\varepsilon_2}\dot{\varepsilon}_2)(F_{iB})_o + (W_{\varepsilon_2})_o\dot{F}_{iB} - C_2(\dot{g}_2)_{i,B}]M_AM_B.\end{aligned} \tag{70}$$

In the case of Neo–Hookean material (Eq. (41)), the above reduces to (e.g. $W_{II} = 0,\ W_{I\varepsilon_1} = 0,\ W_{I\varepsilon_2} = 0$ etc...)

$$\begin{aligned}\dot{P}_{iA} &= 2\mu\dot{F}_{iA} - \dot{p}(F^*_{iA})_o - p_o\dot{F}^*_{iA} + [E_1\dot{\varepsilon}_1(F_{iB})_o + E_1(\varepsilon_1)_o\dot{F}_{iB} - C_1(\dot{g}_1)_{i,B}]L_AL_B\\ &+[E_2\dot{\varepsilon}_2(F_{iB})_o + E_2(\varepsilon_2)_o\dot{F}_{iB} - C_2(\dot{g}_2)_{i,B}]M_AM_B.\end{aligned} \tag{71}$$

Evaluating limits at $\epsilon = 0$, we have

$$\begin{aligned}\dot{P}_{iA} &= 2\mu\dot{F}_{iA} - \dot{p}\delta_{iA} - p_o\dot{F}^*_{iA} + [E_1\dot{\varepsilon}_1\delta_{iB} - C_1(\dot{g}_1)_{i,B}]L_AL_B\\ &+[E_2\dot{\varepsilon}_2\delta_{iB} - C_2(\dot{g}_2)_{i,B}]M_AM_B,\end{aligned} \tag{72}$$

where $p_o = 2\mu$, to recover the initial stress free state at $\epsilon = 0$ (i.e. $P_{iA} = 0$ at $\epsilon = 0$). In addition, we approximate the fiber's extensions as

$$\dot{\varepsilon}_1 = \mathbf{FL}\otimes\mathbf{L}\cdot\dot{\mathbf{F}} \simeq \mathbf{L}\otimes\mathbf{L}\cdot\dot{\mathbf{F}} = \dot{F}_{jC}L_jL_C, \tag{73}$$

and subsequently formulate

$$\begin{aligned}(2\mu\dot{F}_{iA})_{,A} &= 2\mu\dot{F}_{iA,A},\ \ (p_o\dot{F}^*_{iA})_{,A} = 0,\ \ (\dot{p}\delta_{iA})_{,A} = \dot{p}_{,i}\\ (E_1\dot{\varepsilon}_1\delta_{iB}L_AL_B)_{,A} &= (E_1\dot{\varepsilon}_1L_iL_B)_{,A} = E_1\dot{F}_{jA,B}L_iL_jL_AL_B,\ \text{and}\\ (C_1(\dot{g}_1)_{i,B}L_AL_B)_{,A} &= (C_1\dot{F}_{iC,BD}L_CL_DL_AL_B)_{,A} = C_1\dot{F}_{iA,BCD}L_AL_BL_CL_D,\end{aligned} \tag{74}$$

and a similar scheme can be applied for $\dot{\varepsilon}_2$ and $(\dot{g}_2)_i$. Therefore, from Eqs. (69) and (72)–(74), the Euler equation for small deformations is given by

$$\begin{aligned}0 = \dot{P}_{iA,A} &= 2\mu\dot{F}_{iA,A} - \dot{p}_{,i} + E_1\dot{F}_{jA,B}L_iL_jL_AL_B - C_1\dot{F}_{iA,BCD}L_AL_BL_CL_D\\ &+E_2\dot{F}_{jA,B}M_iM_jM_AM_B - C_2\dot{F}_{iA,BCD}M_AM_BM_CM_D,\end{aligned} \tag{75}$$

where we make use of the identities, $Div(\dot{*}) = Div(*)\dot{}$, $(p_o)_{,A} = 0$ and $(\dot{g}_1)_{i,B} = (\dot{F}_{iC,D}L_CL_D)_{,B} = \dot{F}_{iC,BD}L_CL_D$. Alternatively, from Eq. (67), the above can be rewritten as

$$\begin{aligned}\dot{p}_{,i} &= 2\mu u_{i,AA} + E_1u_{j,AB}L_iL_jL_AL_B - C_1u_{i,ABCD}L_AL_BL_CL_D\\ &+E_2u_{j,AB}M_iM_jM_AM_B - C_2u_{i,ABCD}M_AM_BM_CM_D.\end{aligned} \tag{76}$$

We note here that the current and deformed configurations are commuted in the case of superposed incremental deformations (i.e. $\mathbf{e}_\alpha = \mathbf{E}_\alpha$). For an orthonormal family of fibers (i.e. $\mathbf{L} = \mathbf{E}_1,\ L_1 = 1,\ L_2 = 0,\ \mathbf{M} = \mathbf{E}_2,\ M_1 = 0,\ M_2 = 1$), Eq. (76) becomes

$$\dot{p}_{,i} = 2\mu u_{i,AA} + E_1 u_{1,11}\delta_{i1} - C_1 u_{i,1111} + E_2 u_{2,22}\delta_{i2} - C_2 u_{i,2222}. \tag{77}$$

Further, in view of Eqs. (65)–(67), the condition of bulk incompressibility reduces to

$$\dot{(J-1)} = \mathbf{F}_o^* \cdot \dot{\mathbf{F}} = \mathrm{div}\,\mathbf{u} = \mathbf{0}. \tag{78}$$

which, together with the Eq. (76), serves as a compatible form of the equilibrium Eq. (51) for small deformations. Lastly, the boundary conditions in Eq. (60) can be approximated similarly as in the above (e.g. $\mathbf{t} = \mathbf{t}_o + \varepsilon\dot{\mathbf{t}} + o(e)$ etc...),

$$\begin{aligned}
\dot{t}_i &= \dot{P}_{iA}N_A - \frac{d}{dS}[C_1(\dot{g}_1)_i L_A T_A L_B N_B + C_2(\dot{g}_2)_i M_A T_A M_B N_B],\\
\dot{m}_i &= C_1(\dot{g}_1)_i L_A N_A L_B N_B + C_2(\dot{g}_2)_i M_A N_A M_B N_B,\\
\dot{f}_i &= C_1(\dot{g}_1)_i L_A T_A L_B N_B + C_2(\dot{g}_2)_i M_A T_A M_B N_B.
\end{aligned} \tag{79}$$

In particular, if the fiber's directions are either normal or tangential to the boundary (i.e. $(\mathbf{L}\cdot\mathbf{T})(\mathbf{L}\cdot\mathbf{N}) = 0$ and $(\mathbf{M}\cdot\mathbf{T})(\mathbf{M}\cdot\mathbf{N}) = 0$), Eq. (79) yields

$$\begin{aligned}
\dot{t}_i &= \dot{P}_{iA}N_A,\\
\dot{m}_i &= C_1(\dot{g}_1)_i L_A N_A L_B N_B + C_2(\dot{g}_2)_i M_A N_A M_B N_B,\\
\dot{f}_i &= 0,
\end{aligned} \tag{80}$$

where

$$\begin{aligned}
\dot{P}_{iA} &= 2\mu\dot{F}_{iA} - \dot{p}\delta_{iA} - p_o\dot{F}^*_{iA} + E_1\dot{F}_{jB}L_iL_jL_AL_B - C_1(\dot{g}_1)_{i,B}L_AL_B\\
&\quad + E_2\dot{F}_{jB}M_iM_jM_AM_B - C_2(\dot{g}_2)_{i,B}M_AM_B,\\
(\dot{g}_1)_i &= \dot{F}_{iC,D}L_CL_D \text{ and } (\dot{g}_2)_i = \dot{F}_{iC,D}M_CM_D.
\end{aligned} \tag{81}$$

Also, since $J\partial F^*_{jB}/\partial F_{iA} = F^*_{jB}F^*_{iA} - F^*_{iB}F^*_{jA}$ at $\epsilon = 0$, we obtain

$$(\partial F^*_{jB}/\partial F_{iA})_o = \delta_{jB}\delta_{iA} - \delta_{iB}\delta_{jA} \text{ and } (\dot{\mathbf{F}^*_{\mathbf{F}}}[\dot{\mathbf{F}}])_{jB} = (\delta_{jB}\delta_{iA} - \delta_{iB}\delta_{jA})u_{i,A}. \tag{82}$$

Therefore,

$$\dot{F}^*_{iA} = (Div\mathbf{u})\delta_{iA} - u_{A,i} = -u_{A,i}, \tag{83}$$

where $Div\mathbf{u} = \mathrm{div}\,\mathbf{u} = 0$ from the linearized incompressibility condition.

6. Solution to the linearized problem

We introduce scalar field, ϕ, as

$$\mathbf{u} = \mathbf{k}\times\nabla\phi,\ \mathbf{k}(\text{unit normal});\ u_i = \varepsilon_{\lambda i}\phi_{,\lambda}, \tag{84}$$

so that Eq. (78) can be automatically satisfied (i.e. $\phi_{,12} - \phi_{,21} = 0$). Thus, the linearized Euler equation, Eq. (77), furnishes

$$\dot{p}_{,i} = 2\mu\varepsilon_{\lambda i}(\phi_{,\lambda 11} + \phi_{,\lambda 22}) - E_1\phi_{,211}\delta_{i1} - C_1\varepsilon_{\lambda i}\phi_{,\lambda 1111} - E_2\phi_{,122}\delta_{i2} - C_2\varepsilon_{\lambda i}\phi_{,\lambda 2222}. \tag{85}$$

By utilizing the compatibility condition of $\dot{p}_{,i}$ (i.e. $\dot{p}_{,ij} = \dot{p}_{,ji}$), we obtain the following partial differential equation, solving for ϕ,

$$2\mu(\phi_{,1111} + 2\phi_{,1122} + \phi_{,2222}) - C_1(\phi_{,11} + \phi_{,22})_{,1111} - C_2(\phi_{,11} + \phi_{,22})_{,2222} + (E_1 + E_2)\phi_{,1122} = 0. \tag{86}$$

The above further reduces to

$$\Delta[\Delta\phi - \alpha_1\phi_{,1111} - \alpha_2\phi_{,2222}] + (\beta_1 - \beta_2)\phi_{,1122} = 0, \tag{87}$$

where $\alpha_1 = \frac{C_1}{2\mu} > 0,\ \alpha_2 = \frac{C_2}{2\mu} > 0,\ \beta_1 = \frac{E_1}{2\mu} > 0$ and $\beta_2 = \frac{E_2}{2\mu} > 0$. We note here that the solution of Eq. (87) is not accommodated by the conventional methods such as the Fourier transform or the separation of variables. Instead, we adopt the methods of iterative reduction and the principle of eigenfunction expansion, and obtain the potential function for $\phi(x,y)$. Details are reserved for the sake of conciseness, but can be found in Huang and Zhang (2002); Read (1993, 1996). Accordingly, the general solution of Eq. (87) can be obtained as

$$\begin{aligned}
\phi(x,y) = \sum_{m=1}^{\infty}[\{&A_m\exp(xT)\ + B_m\exp(-xT)\ + \exp(a_mx)(C_m\cos b_mx + D_m\ \sin b_m\ x) +\\
&\exp(-a_mx)(E_m\cos b_mx + F_m\ \sin b_m\ x)\} \times (\sin my)],
\end{aligned} \tag{88}$$

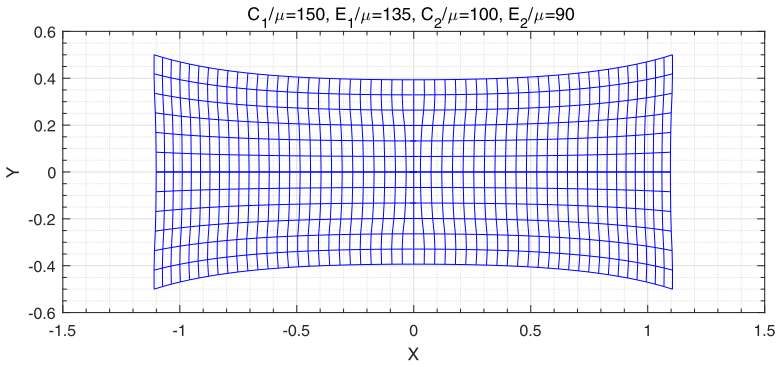

Fig. 13. Deformed configuration under axial loading $P_{11}/\mu = 50$.

where

$$a_m = \sqrt{\frac{\sqrt{\left(\frac{\sqrt{3}}{2}\left(\frac{P}{Q}+Q\right)\right)^2+\left(-\frac{Q}{2}+\frac{P}{2Q}-\frac{B}{3A}\right)^2}+\left(-\frac{Q}{2}+\frac{P}{2Q}-\frac{B}{3A}\right)}{2}},$$

$$b_m = \sqrt{\frac{\sqrt{\left(\frac{\sqrt{3}}{2}\left(\frac{P}{Q}+Q\right)\right)^2+\left(-\frac{Q}{2}+\frac{P}{2Q}-\frac{B}{3A}\right)^2}-\left(-\frac{Q}{2}+\frac{P}{2Q}-\frac{B}{3A}\right)}{2}},$$

$$P = \frac{C}{3A}-\frac{B^2}{9A^2},\ T = \sqrt{Q-\frac{P}{Q}-\frac{B}{3A}},$$

$$Q = \sqrt[3]{\left(\left(\frac{C}{3A}-\frac{B^2}{9A^2}\right)^3+\left(\frac{B^3}{27A^3}+\frac{D}{2A}-\frac{B.C}{6A^2}\right)^2\right)^{\frac{1}{2}}-\frac{B^3}{27A^3}-\frac{D}{2A}+\frac{BC}{6A^2}},$$

and

$$m = \frac{\pi n}{2d},\ A = -\alpha_1,\ B = (1-m^2),\ C = -m^2(\alpha_2 m^2-\beta_1-\beta_2+2),\ D = -m^4(\alpha_2 m^2+1). \tag{89}$$

The unknown constant real numbers A_m, B_m, C_m, D_m, E_m, and F_m can be completely determined by imposing admissible boundary conditions, as depicted in Eqs. (80)–(83). The analytical solution, ϕ, is then converted through the mapping, $\chi = (X_1-\phi_{,2})\mathbf{e}_1+(X_2+\phi_{,1})\mathbf{e}_2$, to obtain the complete deformed configurations (see, for example, Fig. 13). It is also noted here that the corresponding stress fields can also be obtained through Eqs. (81), (84) and (85). For example, in cases of fiber composites subjected to lateral extension and/or flexure (see, Fig. 1), we impose the following boundary conditions from Eqs. (80), (81) and (84):

$$\begin{aligned}&\dot{P}_{11} = 2\mu u_{1,1}-\dot{p}-2\mu u_{2,2}+E_1u_{1,1}-C_1u_{1,111}\text{: extension,}\\ &\dot{\mathbf{m}} = \dot{m}_1\mathbf{e}_1+\dot{m}_2\mathbf{e}_2,\ \dot{m}_1 = C_1u_{1,11}\ \text{and}\ \dot{m}_2 = 0\text{: flexure,}\end{aligned} \tag{90}$$

where $u_{1,1} = -\phi_{,21}$, $u_{1,11} = -\phi_{,211}$, $u_{1,111} = -\phi_{,2111}$ and similarly for u_2 (see, Eq. (84)). In the analysis, the applied tensions and moments are approximated via Fourier series as;

$$\dot{P}_{11} = 2\mu u_{1,1}-\dot{p}-2\mu u_{2,2}+E_1u_{1,1}-C_1u_{1,111} = 50 \approxeq \sum_{l=1}^{30}\frac{200}{\pi l}(-1)^{\frac{l-1}{2}}\cos(\frac{\pi l}{2d})y, \tag{91}$$

and

$$\begin{aligned}&\dot{\mathbf{m}} = \dot{m}_1\mathbf{e}_1+\dot{m}_2\mathbf{e}_2,\ \dot{m}_1 = C_1u_{1,11} = 80 \approxeq \sum_{n=1}^{30}\frac{20}{\pi n}(-1)^{\frac{n-1}{2}}\cos(\frac{\pi n}{2d})y\mathbf{e}_m,\\ &\dot{m}_2 = 0,\end{aligned} \tag{92}$$

which ensure fast convergence (within 30 iterations). Despite the presence of sharp corners, where singular behaviors of response functions are often observed (e.g. discontinuities and oscillations), the obtained solutions are smooth and stable throughout the entire domain of interest (Fig. 13), with reasonable sensitivity of the fibers' resistance to both the extension and the flexure. More precisely, Figs. 14and 15 clearly indicate the inverse correlations between the magnitude of deformations and the fiber's material parameters (i.e. E_1, E_2, C_1, and C_2.).

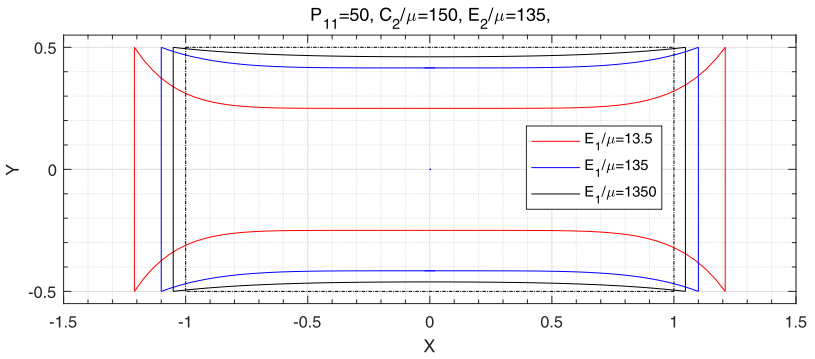

Fig. 14. Deformation profiles with respect to E_1/μ when $P_{11}/\mu = 50$..

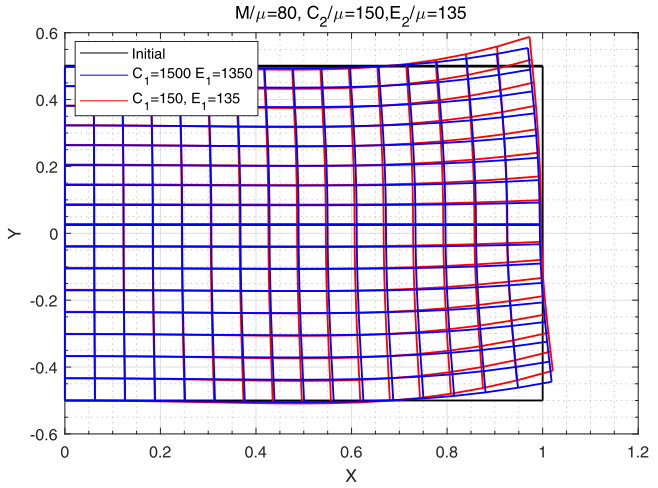

Fig. 15. Deformed configurations with respect to E_1/μ.

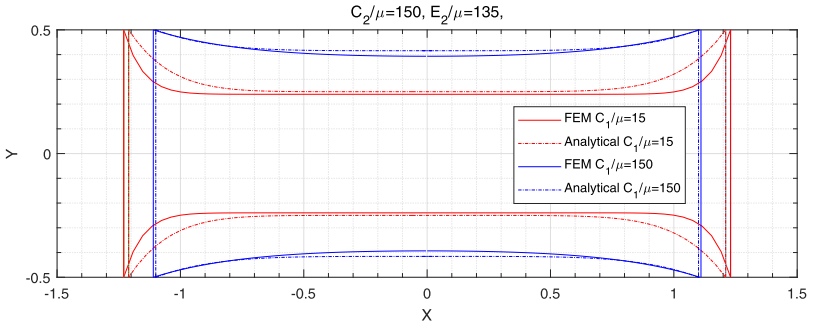

Fig. 16. Linear (Analytical) VS nonlinear (Numerical) solutions: extension P_{11}/μ =50.

In particular, the linear (analytical) solution displays good agreement with the nonlinear solutions (FEA) and experiments (Dong & Davies, 2015) for small deformations superposed on large (see, Figs. 11, 16 and 17), while it demonstrate discrepancies in the predictions of large deformations (see, Figs. 16 and 17). Overall, the proposed models perform well in the analysis of the mechanical behavior of fiber-reinforced composites and therefore they can be easily adopted in the relevant subjects of studies, including experiments. In particular, the one from the linear theory is particularly useful, as it provides an explicit form of solution rather than a discretized solution.

7. Conclusion

In this study, we present a continuum model for the mechanics of an elastic solid reinforced with bidirectional fibers in finite plane elastostatics. The fibers are idealized as continuously distributed spatial rods of the Kirchhoff type, in which

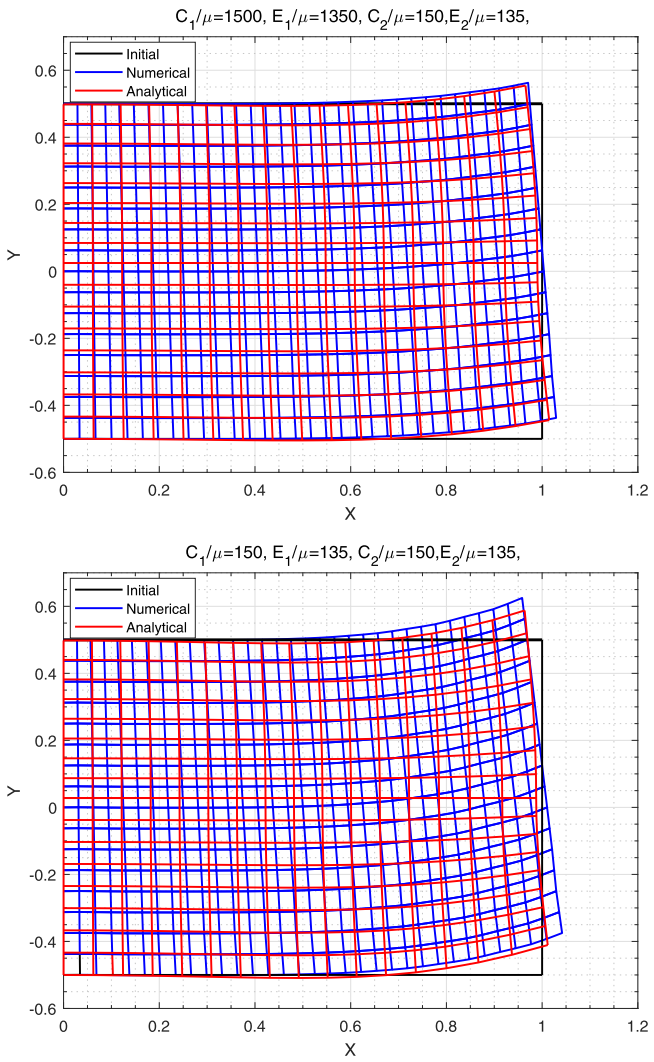

Fig. 17. Linear (Analytical) VS nonlinear (Numerical) solutions: flexure $M/\mu = 50$.

their elastic resistant to stretch and flexure are incorporated into the models of deformations via the first and second gradients of deformations, respectively. Using the variational principles and the virtual work statement, the Euler equation and necessary boundary conditions are derived. These, in turn, leads to a highly nonlinear coupled PDE system from which a set of numerical solutions describing mechanical responses of fiber composites are obtained.

More importantly, we examine the plane bias extensions in the case of fiber-reinforced composites and demonstrate that the proposed model successfully predicts the continuous distributions of shear strain fields through the second gradient of deformations. Within the prescription of superposed incremental deformations, a compatible linear theory, including boundary conditions, is developed and used to obtain complete analytical solutions. The results obtained from the linear theory demonstrate close agreement with the both numerical predictions and experiments for the small deformation regime. Lastly, we mention that the proposed model can be used as an alternative 2D Cosserat theory of non-linear elasticity.

Acknowledgments

This work was supported by the Natural Sciences and Engineering Research Council of Canada via grant #RGPIN 04742 and the University of Alberta through a start-up grant. The author would like to thank Dr. David Steigmann for discussions concerning the underlying theory.

Appendix A. Finite element analysis of the 4th order coupled PDE

It is not trivial to demonstrate numerical analysis procedures for coupled PDE systems, especially for those with high order terms, since the piece-wise linear function adopted in FE analysis has limited differentiability up to the second order. For preprocessing, Eq. (51) can be recast as

$$
\begin{aligned}
0 &= 2\mu(Q+H) - AS + BD - C_1 Q_{,11} - C_2 H_{,22} - \frac{E_1}{2}Q - \frac{E_2}{2}H \\
&\quad + \frac{E_1}{2}(3QC^2 + QD^2 + 2RCD) + \frac{E_2}{2}(3HG^2 + HS^2 + 2TGS), \\
0 &= 2\mu(R+T) + AG - BC - C_1 R_{,11} - C_2 T_{,22} - \frac{E_1}{2}R - \frac{E_2}{2}T \\
&\quad + \frac{E_1}{2}(3RD^2 + RC^2 + 2QDC) + \frac{E_2}{2}(3TS^2 + \chi_{2,22}G^2 + 2HSG), \\
0 &= C\chi_{2,2} - D\chi_{1,2} - 1,\ 0 = Q - \chi_{1,11},\ 0 = R - \chi_{2,11},\ 0 = C - \chi_{1,1},\ 0 = D - \chi_{2,1},\ 0 = T - \chi_{2,22}, \\
0 &= S - \chi_{2,2},\ 0 = G - \chi_{1,2},\ 0 = H - \chi_{1,22}, \\
0 &= A - \mu(\chi_{1,11} + \chi_{1,22}) - CR_{,11},\ 0 = B - \mu(\chi_{2,11} + \chi_{2,22}) - CQ_{,11},
\end{aligned} \tag{92}
$$

where $A = p_{,1}$, $B = p_{,2}$, $Q = \chi_{1,11}$, $R = \chi_{2,11}$, $T = \chi_{2,22}$, $H = \chi_{1,22}$, $C = \chi_{1,1}$, $D = \chi_{2,1}$, $S = \chi_{2,2}$ and $G = \chi_{1,2}$. The above non-linear terms can be treated as, for example,

$$
\begin{aligned}
-A\chi_{2,2} + B\chi_{2,1} &\Rightarrow -A_0\chi_{2,2} + B_0\chi_{2,1}, \\
A\chi_{1,2} - B\chi_{1,1} &\Longrightarrow A_0\chi_{1,2} - B_0\chi_{1,1}, \\
C\chi_{2,2} - D\chi_{2,1} &\Longrightarrow C_0\chi_{2,2} - D_0\chi_{2,1}, \\
3QCC + QDD + 2RCD &\Longrightarrow 3QC_0^2 + QD_0^2 + 2RC_0D_0, \\
3RDD + RCC + 2QDC &\Longrightarrow 3RD_0^2 + RC_0^2 + 2QD_0C_0, \\
3HGG + HSS + 2TGS &\Longrightarrow 3HG_0^2 + HS_0^2 + 2TG_0S_0, \\
3TSS + TGG + 2HSG &\Longrightarrow 3TS_0^2 + TG_0^2 + 2HS_0G_0,
\end{aligned} \tag{93}
$$

where the values of $A, B, C, D, Q, R, T, H, S$ and G continue to be refreshed based on their previous estimations (i.e. A_o, B_o, C_0, D_0, Q_0, R_0, T_0, H_0, S_0 and G_0) as iteration progresses. Thus, the weak form of Eq. (92) is obtained by

$$
\begin{aligned}
0 &= \int_\Omega w_1\Big(2\mu(Q+H) - A_0S + B_0D - C_1Q_{,11} - C_2H_{,22} - \frac{E_1}{2}Q - \frac{E_2}{2}H \\
&\quad + \frac{E_1}{2}(3QC_0^2 + QD_0^2 + 2RC_0D_0) + \frac{E_2}{2}(3HG_0^2 + HS_0^2 + 2TG_0S_0)\Big)d\Omega, \\
0 &= \int_\Omega w_2\Big(2\mu(R+T) + A_0G - B_0C - C_1R_{,11} - C_2T_{,22} - \frac{E_1}{2}R - \frac{E_2}{2}T \\
&\quad + \frac{E_1}{2}(3RD_0^2 + RC_0^2 + 2QD_0C_0) + \frac{E_2}{2}(3TS_0^2 + TG_0^2 + 2HS_0G_0)\Big)d\Omega, \\
0 &= \int_\Omega w_3(C\chi_{2,2} - D\chi_{1,2} - 1)d\Omega,\ 0 = \int_\Omega w_4(Q - \chi_{1,11})d\Omega,\ 0 = \int_\Omega w_5(R - \chi_{2,11})d\Omega,\ 0 = \int_\Omega w_6(C - \chi_{1,1})d\Omega, \\
0 &= \int_\Omega w_7(D - \chi_{2,1})d\Omega,\ 0 = \int_\Omega w_8(T - \chi_{2,22})d\Omega,\ 0 = \int_\Omega w_9(S - \chi_{2,2})d\Omega,\ 0 = \int_\Omega w_{10}(G - \chi_{1,2})d\Omega, \\
0 &= \int_\Omega w_{11}(H - \chi_{1,22})d\Omega,\ 0 = \int_\Omega w_{12}(A - \mu(\chi_{1,11} + \chi_{1,22}) - CR_{,11})d\Omega, \\
0 &= \int_\Omega w_{13}(B - \mu(\chi_{2,11} + \chi_{2,22}) - CQ_{,11})d\Omega,
\end{aligned} \tag{94}
$$

where the unknowns (e. g. χ_1, χ_2, Q_1, R_1, A, B etc...) can be written in the form of Lagrangian polynomial such that $(*) = \sum_{j=1}^{n}[(*)_j\Psi_j(x,y)]$. The corresponding test function w is given by

$$
w = \sum_{i=1}^{n} w_i\Psi_i(x,y), \tag{95}
$$

where w_i is the weight of the test function and $\Psi_i(x, y)$ are the shape functions such that,

$$
\begin{bmatrix} \psi_1 & \psi_5 & \psi_9 & \psi_{13} \\ \psi_2 & \psi_6 & \psi_{10} & \psi_{14} \\ \psi_3 & \psi_7 & \psi_{11} & \psi_{15} \\ \psi_4 & \psi_8 & \psi_{12} & \psi_{16} \end{bmatrix} = \begin{bmatrix} f_1 \\ f_2 \\ f_3 \\ f_4 \end{bmatrix} [g_1 \quad g_2 \quad g_3 \quad g_4], \tag{96}
$$

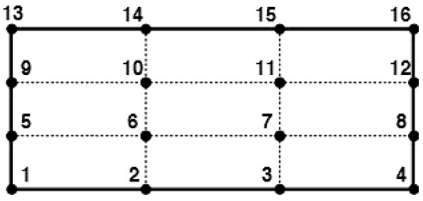

Fig. 18. Schematic of 16 nodes rectangular element.

where

$$f_1(x) = \frac{\left(x-\frac{c}{3}\right)\left(x-\frac{2c}{3}\right)(x-c)}{\left(-\frac{c}{3}\right)\left(-\frac{2c}{3}\right)(-c)}, \quad f_2(x) = \frac{x\left(x-\frac{2c}{3}\right)(x-c)}{\left(\frac{c}{3}\right)\left(-\frac{c}{3}\right)\left(-\frac{2c}{3}\right)},$$

$$f_3(x) = \frac{x\left(x-\frac{c}{3}\right)(x-c)}{\left(\frac{2c}{3}\right)\left(\frac{c}{3}\right)\left(-\frac{c}{3}\right)}, \quad f_4(x) = \frac{x\left(x-\frac{c}{3}\right)\left(x-\frac{2c}{3}\right)}{\left(\frac{c}{3}\right)\left(\frac{2c}{3}\right)(c)}$$

$$g_1(y) = \frac{\left(y-\frac{d}{3}\right)\left(y-\frac{2d}{3}\right)(y-d)}{\left(-\frac{d}{3}\right)\left(-\frac{2d}{3}\right)(-d)}, \quad g_2(y) = \frac{y\left(y-\frac{2d}{3}\right)(y-d)}{\left(\frac{d}{3}\right)\left(-\frac{d}{3}\right)\left(-\frac{2d}{3}\right)},$$

$$g_3(y) = \frac{y\left(y-\frac{d}{3}\right)(y-d)}{\left(\frac{2d}{3}\right)\left(\frac{d}{3}\right)\left(-\frac{d}{3}\right)}, \quad g_4(y) = \frac{y\left(y-\frac{d}{3}\right)\left(y-\frac{2d}{3}\right)}{\left(\frac{d}{3}\right)\left(\frac{2d}{3}\right)(d)}.$$

The assignment of each shape function is illustrated in Fig. 18.

Using Lagrangian polynomial representation, the first of Eq. (94) can be rewritten as

$$\begin{aligned}
0 = &\sum_{i,j=1}^{n}\Big[\int_\Omega (2\mu\Psi_i\Psi_j + C_1\Psi_{i,1}\Psi_{j,1} - \frac{E_1}{2}\Psi_i\Psi_j)d\Omega\Big]Q_j + \sum_{i,j=1}^{n}\Big[\int_\Omega (2\mu\Psi_i\Psi_j + C_2\Psi_{i,2}\Psi_{j,2} - \frac{E_2}{2}\Psi_i\Psi_j)d\Omega\Big]H_j \\
&+ \sum_{i,j=1}^{n}\Big[\int_\Omega A_0\Psi_i\Psi_j d\Omega\Big]S_j - \sum_{i,j=1}^{n}\Big[\int_\Omega B_0\Psi_i\Psi_j d\Omega\Big]D_j + \sum_{i,j=1}^{n}\Big[\frac{E_1}{2}\int_\Omega 3\Psi_i\Psi_j C_0^2\}d\Omega\Big]Q_j + \sum_{i,j=1}^{n}\Big[\frac{E_1}{2}\int_\Omega \Psi_i\Psi_j D_0^2 d\Omega\Big]Q_j \\
&+ \sum_{i,j=1}^{n}\Big[\frac{E_1}{2}\int_\Omega 2\Psi_i\Psi_j C_0 D_0 d\Omega\Big]R_j + \sum_{i,j=1}^{n}\Big[\frac{E_2}{2}\int_\Omega 3\Psi_i\Psi_j S_0^2 d\Omega\Big]H_j + \sum_{i,j=1}^{n}\Big[\frac{E_2}{2}\int_\Omega \Psi_i\Psi_j G_0^2 d\Omega\Big]H_j \\
&+ \sum_{i,j=1}^{n}\Big[\frac{E_2}{2}\int_\Omega 2\Psi_i\Psi_j G_0 S_0 d\Omega\Big]T_j - \int_{\partial\Gamma}(C_1\Psi_i Q_{,1} + C_2\Psi_i H_{,2})N d\Gamma,
\end{aligned} \tag{97}$$

and similarly for the rest of equations. In the above, Ω, $\partial\Gamma$ and $\mathbf{N}$ are respectively, the domain of interest, the associated boundary, and the rightward unit normal to the boundary $\partial\Gamma$ in the sense of the Green–Stoke's theorem. Finally, we obtain the systems of equations $[\mathbb{K}][\mathbb{E}] = [\mathbb{F}]$, where $[\mathbb{K}]$ and $[\mathbb{F}]$ are $[13\times 12]$ and $[12\times 1]$ matrices and $[\mathbb{E}]$ is $[13\times 1]$ matrix with unknowns (e. g. χ_1, χ_2, Q_1, R_1, A, B etc...), respectively. The expressions of $[K^{ij}]$ and $[F_i]$ can be obtained via the standard Finite Element Analysis procedures. For example,

$$\left[K^{11}\right] = \int_\Omega [2\mu\Psi_i\Psi_j + C_1\Psi_{i,1}\Psi_{j,1} - \frac{E_1}{2}\Psi_i\Psi_j + \frac{E_1}{2}(3\Psi_i\Psi_j C_0^2 + \Psi_i\Psi_j D_0^2)]d\Omega,$$

and

$$F_1 = -\int_{\partial\Gamma}(C_1\Psi_i Q_{,1} + C_2\Psi_i H_{,2})N d\Gamma.$$

Supplementary material

Supplementary material associated with this article can be found, in the online version, at 10.1016/j.ijengsci.2018.06.002

References

Antman, S. S. (2005). *Nonlinear problems of elasticity*. Berlin: Springer.

Cuomo, M., dell'Isola, F., & Greco, L. (2016). Simplified analysis of a generalized bias-test for fabricswith two families of inextensible fibres. *The Zeitschrift fur Angewandte Mathematik und Physik, 39*. doi:10.1007/s00033-016-0653-z.

dell'Isola, F., Cuomo, M., Greco, L., & Della Corte, A. (2017). Bias extension test for pantographic sheets: numerical simulations based on second gradient shear energies. *The Journal of Engineering Mathematics, 103*(1), 127–157. doi:10.1007/s10665-016-9865-7.

dell'Isola, F., Della Corte, A., Greco, L., & Luongo, A. (2016). Plane bias extension test for a continuum with two inextensible families of fibers: A variational treatment with lagrange multipliers and a perturbation solution. *The International Journal of Solids and Structures, 81*, 1–12. doi:10.1016/j.ijsolstr.2015.08.029.

Dell'Isola, F., Giorgio, I., Pawlikowski, M., & Rizzi, N. L. (2016). Large deformations of planar extensible beams and pantographic lattices: Heuristic homogenization, experimental and numerical examples of equilibrium. *Proceedings of the Royal Society A, 472*(2185).
Dill, E. H. (1992). Kirchhoff'S theory of rods. *Archive for History of Exact Sciences, 44*, 1–23.
Dong, C., & Davies, I. J. (2015). Flexural strength of bidirectional hybrid epoxy composites reinforced by e glass and t700s carbon fibres. *Composites: Part B, 72*, 65–71.
Fried, E., & Gurtin, M. E. (2009). Gradient nanoscale polycrystalline elasticity: intergrain interactions and triple-junction conditions. *Journal of the Mechanics and Physics of Solids, 57*, 1749–1779.
Germain, P. (1973). The method of virtual power in continuum mechanics, part 2: Microstructure. *SIAM Journal on Applied Mathematics, 25*, 556–575.
Hahm, S. W., & Khang, D. Y. (2010). Crystallization and microstructure-dependent elastic moduli of ferroelectric p(VDF-trFE) thin films. *Soft Matter, 6*, 5802–5806.
Huang, Y., & Zhang, X. (2002). General analytical solution of transverse vibration for orthotropic rectangular thin plates. *Journal of Marine Science and Application, 1*(2), 78–82.
Koiter, W. T. (1964). Couple-stresses in the theory of elasticity. *Proceedings of the Koninklijke Nederlandse Akademie Van Wetenschappen B, 67*, 17–44.
Landau, L. D., & Lifshitz, E. M. (1986). *Theory of elasticity* (3rd). Oxford: Pergamon.
Maugin, G. A., & Metrikine, A. V. (2010). *Mechanics of generalized continua: One hundred years after the cosserats*. New York: Springer.
Mindlin, R. D., & Tiersten, H. F. (1962). Effects of couple-stresses in linear elasticity. *The Archive for Rational Mechanics and Analysis, 11*, 415–448.
Monecke, J. (1989). Microstructure dependence of material properties of composites. *Physica Status Solidi (b), 154*, 805–813.
Moravec, F., & Holecek, M. (2010). Microstructure-dependent nonlinear viscoelasticity due to extracellular flow within cellular structures. *International journal of solids and structures, 47*, 1876–1887.
Mulhern, J. F., Rogers, T. G., & Spencer, A. J. M. (1967). A continuum model for fibre-reinforced plastic materials. *Proceedings of the Royal Society of London A., 301*.
Mulhern, J. F., Rogers, T. G., & Spencer, A. J. M. (1969). A continuum theory of a plastic–elastic fibre-reinforced material. *The International Journal of Engineering Science, 7*, 129–152. doi:10.1016/0020-7225(69)90053-6.
Munch, I., Neff, P., & Wagner, W. (2011). Transversely isotropic material: Nonlinear cosserat vs classical approach. *Continuum Mechanics and Thermodynamics, 23*, 27–34.
Neff, P. (2006a). Existence of minimizers for a finite-strain micro-morphic elastic solid. *Proceedings of the Royal Society of Edinburgh Section A, 136*, 997–1012.
Neff, P. (2006b). A finite-strain elastic–plastic cosserat theory for polycrystals with grain rotations. *The International Journal of Engineering Science, 44*, 574–594. doi:10.1016/j.ijengsci.2006.04.002.
Ogden, R. W. (1984). Non-linear elastic deformations. *Ellis Horwood ltd*. England: Chichester.
Park, H. C., & Lakes, R. S. (1987). Torsion of a micropolar elastic prism of square cross section. *The International Journal of Solids and Structures, 23*, 485–503.
Park, S. K., & Gao, X. L. (2008). Variational formulation of a modified couple-stress theory and its application to a simple shear problem. *The Zeitschrift fur Angewandte Mathematik und Physik, 59*, 904–917.
Pietraszkiewicz, W., & Eremeyev, V. A. (2009). On natural strain measures of the non-linear micropolar continuum. *The International Journal of Solids and Structures, 46*, 774–787.
Pipkin, A. C. (1979). Stress analysis for fiber-reinforced materials. *Advances in Applied Mechanics, 19*, 1–51. doi:10.1016/S0065-2156(08)70308-9.
Pipkin, A. C., & Rogers, T. G. (1971). Plane deformations of incompressible fiber-reinforced materials. *ASME Journal of Applied Mechanics, 38*(8), 634–640. doi:10.1115/1.3408866.
Read, W. W. (1993). Series solutions for laplace's equation with nonhomogeneous mixed boundary conditions and irregular boundaries. *Mathematical and Computer Modelling, 17*(12), 9–19.
Read, W. W. (1996). Analytical solutions for a helmholtz equation with dirichlet boundary donditions and arbitrary boundaries. *Mathematical and Computer Modelling, 24*(2), 23–34.
Reissner, E. (1987). A further note on finite-strain force and moment stress elasticity. *The Zeitschrift fur Angewandte Mathematik und Physik, 38*, 665–673.
Spencer, A. J. M. (1972). *Deformations of fibre-Reinforced materials*. Oxford University Press.
Spencer, A. J. M., & Soldatos, K. P. (2007). Finite deformations of fibre-reinforced elastic solids with fibre bending stiffness. *International Journal of Non-Linear Mechanics, 42*, 355–368. doi:10.1016/j.ijnonlinmec.2007.02.015.
Steigmann, D. J. (2012). Theory of elastic solids reinforced with fibers resistant to extension, flexure and twist. *The International Journal of Non-Linear Mechanics, 47*, 734–742. doi:10.1016/j.ijnonlinmec.2012.04.007.
Steigmann, D. J., & dell'Isola, F. (2015). Mechanical response of fabric sheets to three-dimensional bending, twisting, and stretching. *Acta Mechanica Sinica, 31*(3), 373–382. doi:10.1007/s10409-015-0413-x.
Toupin, R. A. (1964). Theories of elasticity with couple stress. *The Archive for Rational Mechanics and Analysis, 17*, 85–112.
Truesdell, C., & Noll, W. (1965). The non-linear field theories of mechanics. In S. Flugge (Ed.), *Handbuch der physik, vol. III/3*. Berlin: Springer.
Turco, E., et al. (2016). Non-standard coupled extensional and bending bias tests for planar pantographic lattices. *Part I: numerical simulations. The Zeitschrift fur Angewandte Mathematik und Physik, 67*(5), 122.
Voigt, W. (1887). Theoretical studies on the elasticity relationships of crystals. *Abh. Gesch. Wiss., 34*.
Zeidi, M., & Kim, C. (2017a). Finite plane deformations of elastic solids reinforced with fibers resistant to flexure: Complete solution. *Archive of Applied Mechanics*. doi:10.1007/s00419-018-1344-3.
Zeidi, M., & Kim, C. (2017b). Mechanics of fiber composites with fibers resistant to extension and flexure. *Mathematics and Mechanics of Solids*. doi:10.7939/R3Z892V17.
Zeidi, M., & Kim, C. (2018). Mechanics of an elastic solid reinforced with bidirectional fiber in finite plane elastostatics: Complete analysis. *Continuum Mechanics and Thermodynamics*. doi:10.1007/s00161-018-0623-0.